Numerical Modeling of Li-ion Battery Electrode Materials with Phase Interfaces

By

Sungick Kim

A dissertation submitted in partial fulfillment
of the requirements for the degree of
Doctor of Philosophy
(Mechanical Engineering)
in the University of Michigan
2011

Doctoral Committee:

Associate Professor Krishnakumar R. Garikipati, Chair
Professor Anna G. Stefanopoulou
Assistant Professor Vikram Gavini
Assistant Professor Anton Van der Ven

2011

To my parents, sister, and niece

TABLE OF CONTENTS

LIST OF TABLES

LIST OF FIGURES

ABSTRACT

Intercalation processes occur in a single crystallite of many electrode materials for a certain period of charging and discharging processes of primary or secondary batteries. These intercalation processes involve both phase transformation and diffusion. As Li atoms are added to or taken out of the crystallite during the (de)intercalation process, the crystallite relaxes to achieve minimum energy morphology while often having sharp interfaces between two dissimilar phases. Since the two phases have different mechanical properties, especially different lattice parameters, this discrepancy in the lattice parameters near the phase-interfaces causes coherency strain. The resulting coherency strain affects thermodynamic potentials. Conversely the changed thermodynamic potentials vary solubility limits of Lithium, voltage profile, and phase stability.

Although the importance of coherency strain has been noticed by many authors, the effect of coherency strain on two-phase equilibrium has not been modeled to satisfactory degrees for the Li_xFePO_4 crystallite. We analytically derived chemical and mechanical equilibrium criteria for 2-phase morphology of the Li_xFePO_4 crystallites in the quasi-static analysis. We checked the effect of coherency strain on the voltage profile and on the optimal shape of the crystallites. Quasi-static FEA showed that needle-shape crystallite along the a-axis of the Li_xFePO_4 crystallite minimized the

coherency strain energy density. For olivine Li_xFePO_4 ($0 \leq x \leq 1$) crystallite, by adding the coherency strain energy term to the total free energy, we confirmed that the total energy is minimized when the phase interface parallels the bc-plane, although the Li ions diffuse along the b-axis of the crystallite.

In the time dependent analysis, not only the anisotropy of the elastic moduli, but also the anisotropy of the diffusivity was considered. The evolution of the two-phase interface was modeled with the Level set method, one of most accurate and efficient methods to track a surface evolution. We showed a general time-dependent finite element approach for Li-ion battery electrode materials demonstrating Li intercalation processes with the phase interfaces.

CHAPTER I

Introduction

1. 1. Background of Coupled Physics of Li-ion Battery Electrodes

Intercalation processes occur in a single crystallite of many electrode materials for a certain period of the charging and discharging processes of primary or secondary batteries. This intercalation process involves both diffusion and first order phase transformations [1-6]. Because of the phase transformation, many electrode materials for Lithium-ion batteries have been shown to have moving interfaces between two phase portions. For most of the electrode materials in lithium ion batteries, the thickness of transition zones between two phase portions are infinitesimal compared to the dimensions of typical mid-size electrode crystallites: e.g. 4∼6 nm transition zone for Li_xFePO_4 ($0 \le x \le 1$) [7]. Usually insertion or removal of Lithium ions results in slight structural changes of the host because of the changes in the lattice parameters. Also, the resulting coherency strain near the interface affects thermodynamic potentials. Conversely, the changed thermodynamic potentials could vary the solubility limits of the Lithium, voltage profile, and phase stability.

This (de)intercalation kinetics in the electrode materials of Lithium-ion batteries can be treated as a coupled problem of Lithium diffusion and two-phase coherent stress equilibrium. When the (de)intercalation kinetics is modeled as a fully time-dependent

process, tracking the location of the thin interface is necessary and needs to be backed up by numerical schemes that can depict the interface evolution. In this thesis, we adopt the Level Set Method to follow the location of the interface [8].

1. 1. 1. Transport Problem

Anisotropic diffusion in Li_xFePO_4 is treated with the diffusion equation by setting diffusivity tensor properly so that one-dimensional diffusion along b-direction (space group *Pnma*) is guaranteed. The b-direction faces outwards from the surface of the crystallite in Figure 1.1. One-dimensional diffusion in Li_xFePO_4 was elucidated by electron microscopy study of Li_xFePO_4 by G. Chen et al. [7] and was confirmed by D. Morgan, A. Van der Ven, and G. Ceder through first principal calculation [9]. The related governing equation is known as Fick's second law.

$$\frac{\partial x^{\xi}}{\partial t} = -\nabla \cdot j^{\xi} \tag{1.1}$$

where $\xi = \alpha, \beta$. The flux in j^{ξ} in Eq. (1.1) is defined as

$$j^{\xi} = -D^{\xi} \nabla x^{\xi} \tag{1.2}$$

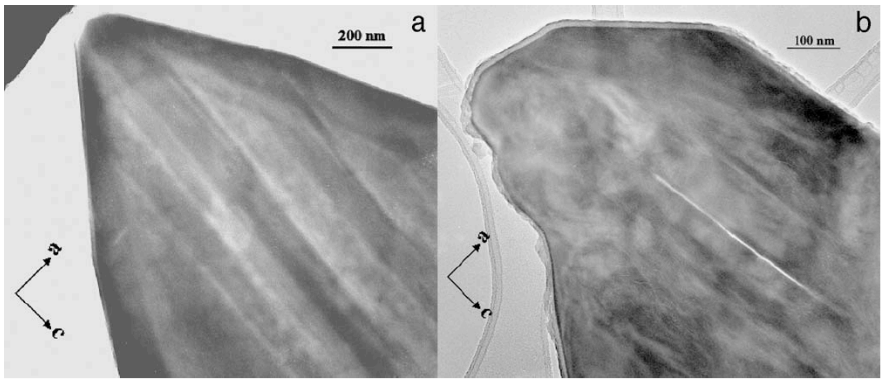

Figure 1.1. TEM images of $Li_{0.5}FePO_4$
(a) aligned along the c-axis, (b) thin crystallite with crack in the bc-plane [7]

1. 1. 2. Stress equilibrium

The momentum balance equation takes care of the effect of strain discontinuity from the lattice mismatch of two dissimilar anisotropic materials at the two-phase interface. Regarding the momentum balance equation, a natural boundary condition applies for all boundaries to Eq. (1.3), since we consider an isolated ideal single crystallite.

$$= 0 \tag{1.3}$$

1. 1. 3. Two-Phase Interface Tracking

To track the position of the thin interface between the two phase portions for the time dependent analysis, we adopt the Level Set Method (LSM). LSM was developed by Stanley Osher and James Sethian to track interface evolutions [8]. With the interface velocity, *v*, calculated from the concentration jump condition and flux jump condition, an advection equation

$$\frac{\partial \phi}{\partial t} + v \cdot \nabla \phi = 0 \tag{1.4}$$

is solved and the zero contour of the solution indicates the evolving interface. Because of numerical unstableness of the advection equation, a numerical stabilizing scheme, Streamlined Upwind Petrov-Galerkin (SUPG) method is added to Eq. (1.4).

1. 2. Review of Related Studies

D. Morgan, A. Van der Ven, and G. Ceder [9] confirmed that Lithium ion diffusion in Li_xFePO_4 ($0 \le x \le 1$) is restricted to one dimensional channels parallel to the b-direction, as illustrated in Figure (1. 2). However, contrary to intuition, the interface is perpendicular to the a-direction not to the b-direction, which was discovered in transmission electron microscopy (TEM) observation by Chen et al. [7] Chen et al. argued that this interface orientation should minimize strain energy. Meethong et al. also showed the importance of misfit strains on the rate capabilities of $LiFePO_4$ crystallites. They showed that nucleation and growth kinetics depend on the misfit strains between two phase portions of $LiFePO_4$. They compared two morphologies and concluded that spherical crystallites with spherical cap has far less strain energy compared to the core/shell model.

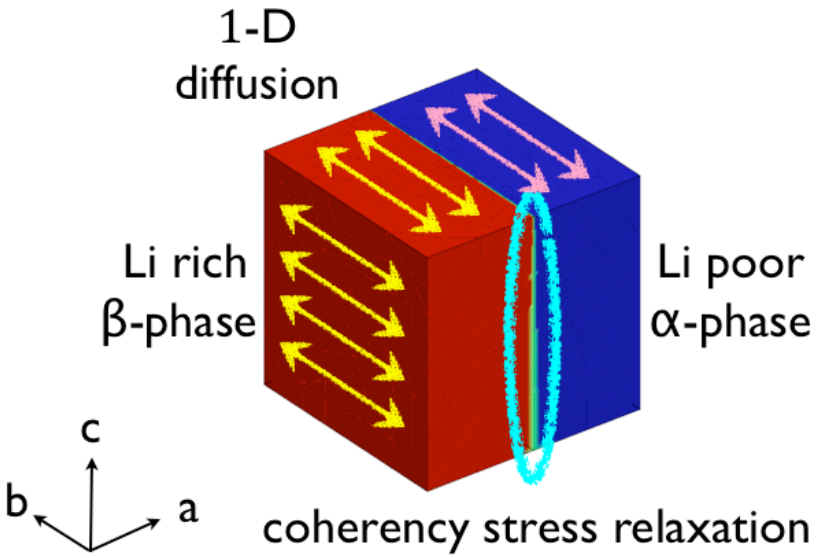

Figure 1.2. One-dimensional diffusion along b-axis and coherency strain near the two-phase interface of Li_xFePO_4

1. 3. Motivation for Research

Many authors have recognized that coherency strains play an important role in determining two-phase equilibrium, which was made evident by the discovery of Chen et al. [7] However, rarely in their papers have they considered coherency strains explicitly for (de)intercalation kinetics.

Past work on the coherent equilibrium of Li-ion electrodes is that the materials also fails to investigate the materials as interstitial solids but as substitutional solids instead, even though intercalation compounds should be viewed as interstitial solids [10, 11].

Moreover, fully time dependent three-dimensional modeling using FE for Li-ion battery electrode materials have not been tried to a satisfactory degree. Lithium (de)

intercalation process is an intrinsically non-equilibrium time dependent phenomenon. Therefore deeper understanding of the (de)intercalation process could be gained from time dependent analysis. An interesting challenge of implementing a time dependent approach is how to track the moving interface between two phase portions. In this thesis, we track the interface adopting the well-known Level Set Method [8].

1. 4. Thesis outline

In Chapter II, the quasi-static analysis is developed. We derive mechanical and chemical equilibrium criteria and applied them to a single crystallite of olivine Li_xFePO_4. We describe how misfit strains or coherency strains regulate solubility limits and add hysteresis in the voltage curve. The effect of coherency strains on overpotential and underpotential is shown to initiate evolution of the coherency crystallite. In the case of Li_xFePO_4, we confirm that an interface orientation perpendicular to the a-direction minimizes free energy. As a final result of quasi-static analysis, we show that a needle-shape crystallite with the longest direction parallel to the a-direction minimizes the strain energy due to the two-phase coexistence in the Li_xFePO_4 crystallite. This optimum shape reduces overpotential as well as the mechanical damage during charge-discharge cycles.

In Chapter III, we describe the role of the coherency strain in time dependent analysis. Through fully time dependent three-dimensional finite element model, we describe the non-equilibrium (de)intercalation process, and thereby hope that we contribute to the fundamental understanding of (de)intercalation kinetics in the Li-ion battery electrode materials.

In Chapter IV, we summarize the findings, draw conclusion, and suggest directions of future work.

CHAPTER II

Quasi-Static Analysis of $LiFePO_4$ Cathode Material

In Chapter II, we will rigorously derive two-phase coexistence equilibrium criteria and will apply the criteria to Li_xFePO_4 cathode material. FE analysis will be conducted on the base of the derivation in the section 2.1 and will be compared with analytic calculation. As a final result of FE analysis, we will show that a needle-shape crystallite with the longest direction parallel to first direction minimizes the strain energy due to two-phase coexistence in section 2.5. This Chapter is based on the paper written by A. Van der Ven, K. Garikipati, S. Kim, and M. Wagemaker [12].

2. 1. Mathematical Formulation

We consider a crystallite having a shape of rectangular prism with 2 coexisting phases, Li-poor α–phase and Li-rich β-phase, as illustrated in Fig. 2.1. Because of two-phase coexistence with crystallographic continuity at the interface and because of different equilibrium dimensions, two phases are stretched or compressed in the 2- and 3-directions at the interface between the coexisting phases. Since the crystal is not constrained on the surfaces perpendicular to the first direction, it can fully relax in that direction with $\sigma_1 = 0$. So we can reduce the problem as a plane stress description.

We set phase fraction of each portion as ϕ^{α} and ϕ^{β}. When setting M as total number of Li interstitial sites within the crystallite, then the number of interstitial sites within α–phase and within β–phase portion is $M\phi^{\alpha}$ and $M\phi^{\beta}$ respectively. We take N as total number of Lithium ion within the crystallite. Then we set N^{α} and $N^{\beta}(= N\text{-}N^{\alpha})$ as the number of Lithium ion within α-phase and the number of Lithium ion within β–phase portion respectively. Thus Lithium concentration within α-phase is calculated as $x^{\alpha} = N^{\alpha}/M\phi^{\alpha}$ and Lithium concentration within β-phase portion is $x^{\beta} = N^{\beta}/M\phi^{\beta}$. Overall Lithium concentration within the crystallite is $x = N/M$.

$$x = \varphi^{\alpha}x^{\alpha} + \varphi^{\beta}x^{\alpha} \tag{2.1}$$

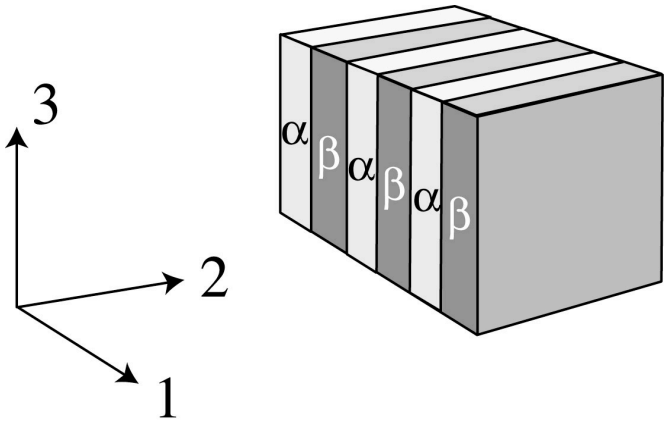

Figure 2.1. Definition of the coordination system for the periodic two phase in orthorhombic crystallite

The dimension of the crystallite depends on Lithium concentration and phase fraction. We define total strains, as written in Eq. (2.2), relative to the dimensions of the single-phase crystallite at equilibrium when $x = 0$, viz., the dimensions of $FePO_4$. In Eq. (2.2), L_i

is a deformed length along *i*-direction, and L^0_i corresponds to reference undeformed length when $x = 0$.

$$\tilde{\varepsilon}_i = \frac{L_i - L_i^0}{L_i^0} \tag{2.2}$$

where $i = 1,2$, and 3.

Following conventional notation, we make 2nd order strain tensor to a vector as below.

$\tilde{\varepsilon}_1 = \tilde{\varepsilon}_{11}$, $\tilde{\varepsilon}_2 = \tilde{\varepsilon}_{22}$, $\tilde{\varepsilon}_3 = \tilde{\varepsilon}_{33}$, $\tilde{\varepsilon}_4 = \tilde{\varepsilon}_{23} = \tilde{\varepsilon}_{32}$, $\tilde{\varepsilon}_5 = \tilde{\varepsilon}_{13} = \tilde{\varepsilon}_{31}$, and $\tilde{\varepsilon}_6 = \tilde{\varepsilon}_{12} = \tilde{\varepsilon}_{21}$.

Total strain, $\tilde{\varepsilon}_i$, is expressed as a change relative to the equilibrium volume of a single phase crystallite having a concentration $x = 0$. The total strains are composed of swelling strain and purely elastic strain. A dimensional change from swelling as Lithium ions are added is denoted by swelling strain, ε_i^0. The elastic strain from external stresses or coherency constraints is ε_i.

$$\tilde{\varepsilon}_i = \varepsilon_i^0(x) + \varepsilon_i \tag{2.3}$$

For only purely elastic strain, we use commonly used generalized Hooke's law for orthotropic symmetry material. Each term of coefficient matrix for Li_xFePO_4 has been determined by first principles analysis by T. Maxisch and G. Ceder [13].

$$\begin{pmatrix} \sigma_1 \\ \sigma_2 \\ \sigma_3 \\ \sigma_4 \\ \sigma_5 \\ \sigma_6 \end{pmatrix} = \begin{bmatrix} c_{11} & c_{12} & c_{13} & 0 & 0 & 0 \\ c_{21} & c_{22} & c_{23} & 0 & 0 & 0 \\ c_{31} & c_{32} & c_{33} & 0 & 0 & 0 \\ 0 & 0 & 0 & 2c_{44} & 0 & 0 \\ 0 & 0 & 0 & 0 & 2c_{55} & 0 \\ 0 & 0 & 0 & 0 & 0 & 2c_{66} \end{bmatrix} \begin{pmatrix} \varepsilon_1 \\ \varepsilon_2 \\ \varepsilon_3 \\ \varepsilon_4 \\ \varepsilon_5 \\ \varepsilon_6 \end{pmatrix} \tag{2.4}$$

Total free energy for the coherent crystallite including the strain energy penalty is

$$G = \phi^{\alpha} M \cdot g^{\alpha}\left(x^{\alpha}\right) + \phi^{\beta} M \cdot g^{\beta}\left(x^{\beta}\right) + E^{strain} \tag{2.5}$$

The total free energy, G, is sum of the free energies of α- and β-phases in their equilibrium dimensions without coherency constraints, and the total elastic energy, arising from coherency strains. $g^{\alpha}(x^{\alpha})$ and $g^{\beta}(x^{\beta})$ are the free energies per unit cell of the homogeneous α- and β-phases. Since the crystal structure of the host is unchanged with Lithium concentration, the free energy of Li_xFePO_4 per unit cell, $g^{\xi}(x^{\xi})$, is continuous function of the Lithium concentration, where $\xi = \alpha$ and β. In Eq. (2.5), the strain energy is total elastic energy of the crystallite arising from coherency strain. We neglect surface and interfacial free energy terms which is of importance for small crystallites. However, the neglected terms are relatively small compared to the volume contributions for a large crystallites.

Assuming homogeneous strains, we calculate an expression for the strain energy analytically. The strain energy is calculated as below.

$$E^{elastic} = \frac{1}{2}\int_{V_0} [\sigma_2\varepsilon_2 + \sigma_3\varepsilon_3]dV_0 = \frac{1}{2}\int_{V_0} \left[\tilde{c}_{22}(\varepsilon_2)^2 + 2\tilde{c}_{23}(\varepsilon_2 \cdot \varepsilon_3) + \tilde{c}_{33}(\varepsilon_3)^2\right]dV_0 \tag{2.6}$$

where the plane stress elastic moduli is

$$\tilde{c}_{ij} = c_{ij} - \frac{c_{1i}c_{1j}}{c_{11}} \tag{2.7}$$

and i = 2 and 3. Detailed derivation of Eq. (2.7) is shown in the Appendix A. The elastic constants, in principle, depend on the Lithium concentration. Since the crystallite is free to relax in a-direction, σ_1 is zero. So there is no term related to σ_1 in Eq. (2.6). Assuming uniform strain in each phase, Eq. (2.6) is simplified to

$$E^{elastic} = V_0\left(\phi^{\alpha}e^{\alpha}\left(\varepsilon_2^{\alpha},\varepsilon_3^{\alpha}\right) + \phi^{\beta}e^{\beta}\left(\varepsilon_2^{\beta},\varepsilon_3^{\beta}\right)\right) \tag{2.8}$$

In Eq.(2.8), e^{ξ} is a strain energy density of each phase:

$$e^{\xi}\left(\varepsilon_2,\varepsilon_3\right) = \frac{1}{2}\left[\tilde{c}_{22}\left(\varepsilon_2^{\xi}\right)^2 + 2\tilde{c}_{23}\left(\varepsilon_2^{\xi}\cdot\varepsilon_3^{\xi}\right) + \tilde{c}_{33}\left(\varepsilon_3^{\xi}\right)^2\right] \tag{2.9}$$

where $\xi = \alpha$ and β.

We write the total free energy per interstitial site of two-phase coexistence material as

$$\tilde{g}_{coex} = \frac{G}{M} = \phi^{\alpha}\tilde{g}^{\alpha} + \phi^{\beta}\tilde{g}^{\beta} \tag{2.10}$$

where

$$\tilde{g} = g(x) + \Omega e(\varepsilon_2, \varepsilon_3) \tag{2.11}$$

$\tilde{g}$ can be interpreted as the free energy of a homogeneous crystallite per interstitial site having concentration x when the crystallite is elastically strained in the 2 and 3 directions by ε_2 and ε_3 but free to relax in the 1 direction. So the free energy for the strained crystallite explicitly depends on temperature T, the pressure P, the Lithium concentration x, and the total strains $\tilde{\varepsilon}_2$ and $\tilde{\varepsilon}_3$, *i.e.*, $\tilde{g}(T, P, x, \varepsilon_2, \varepsilon_3)$. We take $P = 0$ to avoid the Legendre transforms, which is a reasonable approximation for solids at ambient conditions.

We consider a crystallite at constant temperature T, at constant pressure $P = 0$, and with constant number of Lithium ions N. The crystallite has several degree of freedom that are not fixed by external boundary conditions. Although we fix total number of Lithium ion, there distribution over the coexisting phases is not. We can take N^{α} independent ($N^{\beta} = N - N^{\alpha}$). Also one of the phase portions ϕ^{α} is independent ($\phi^{\beta} = 1 -$

ϕ^{α}) and strains in two directions are controllable. Thus, in the Eq. (2.5), we choose four independent variables: N^{α} ,ϕ^{α}, $\tilde{\varepsilon}_2$ and $\tilde{\varepsilon}_3$.

To find equilibrium criteria, we minimize the Gibbs free energy with respect to the four chosen variables. This minimum can be determined by setting the partial derivatives of *G* in Eq. (2.5).

$$\left(\frac{\partial G}{\partial N^{\alpha}}\right)_{\phi^{\alpha}\,\tilde{\varepsilon}_2\,\tilde{\varepsilon}_3} = 0 \tag{2.12}$$

$$\left(\frac{\partial G}{\partial \phi^{\alpha}}\right)_{N^{\alpha}\,\tilde{\varepsilon}_2\,\tilde{\varepsilon}_3} = 0 \tag{2.13}$$

$$\left(\frac{\partial G}{\partial \tilde{\varepsilon}_2}\right)_{N^{\alpha},\phi^{\alpha}\,\tilde{\varepsilon}_3} = 0 \tag{2.14}$$

$$\left(\frac{\partial G}{\partial \tilde{\varepsilon}_3}\right)_{N^{\alpha},\phi^{\alpha}\,\tilde{\varepsilon}_2} = 0 \tag{2.15}$$

The corresponding results are Eq. (2.16) - Eq. (2.19). Detailed derivation is shown in Appendix A.

$$\tilde{\mu}^{\alpha} = \tilde{\mu}^{\beta} \tag{2.16}$$

$$\tilde{g}^{\alpha} - x_{\alpha}\tilde{\mu}^{\alpha} = \tilde{g}^{\beta} - x_{\beta}\tilde{\mu}^{\beta} \tag{2.17}$$

$$\phi^{\alpha}\sigma_2^{\alpha} + \phi^{\beta}\sigma_2^{\beta} = 0 \tag{2.18}$$

$$\phi^{\alpha}\sigma_3^{\alpha} + \phi^{\beta}\sigma_3^{\beta} = 0 \tag{2.19}$$

The first two equations of equilibrium criteria coincide with the common tangent law. For our special case with miscibility gap, the common tangent law means that concentrations of the two stable phases lie on the common tangent to the curve of free energy per unit volume, which is illustrated in Fig 2.2. Specifically, Eq. (2.16) specifies that the slopes are equal, and Eq. (2.17) specifies that the intercepts on the ordinate are equal. The rest two equations, Eq. (2.18) and (2.19), imply that average stresses along b-direction and c-direction are zeros. Since free energy has strain energy term, chemical potential in Eq. (2.16) is derived like Eq. (2.20) and Eq. (2.21), where $\xi = \alpha$ and β.

$$\tilde{\mu}^{\xi} = \left(\frac{\partial \tilde{g}^{\xi}}{\partial x^{\xi}} \right)_{\tilde{\varepsilon}_2, \tilde{\varepsilon}_3} \tag{2.20}$$

$$\tilde{\mu}^{\xi} = \frac{\partial g^{\xi}}{\partial x^{\xi}} + \frac{\Omega}{2}\left[\left(\varepsilon_2^{\xi}\right)^2 \frac{\partial \tilde{c}_{22}^{\xi}}{\partial x^{\xi}} + 2\left(\varepsilon_2^{\xi} \cdot \varepsilon_3^{\xi}\right) \frac{\partial \tilde{c}_{23}^{\xi}}{\partial x^{\xi}} + \left(\varepsilon_3^{\xi}\right)^2 \frac{\partial \tilde{c}_{33}^{\xi}}{\partial x^{\xi}} \right] - \Omega \sum_{i=2}^{3} \frac{\partial e^{\xi}}{\partial \varepsilon_i^{\xi}} \frac{\partial \varepsilon_i^{0\xi}}{\partial x^{\xi}} \tag{2.21}$$

Since stress can be expressed as

$$\sigma_i^{\xi} = \left(\frac{\partial e^{\xi}}{\partial \varepsilon_i^{\xi}} \right)_{x^{\xi}, \tilde{\varepsilon}_{j \neq i}} = \left(\frac{\partial \tilde{g}^{\xi}}{\partial \tilde{\varepsilon}_i^{\xi}} \right)_{x^{\xi}, \tilde{\varepsilon}_{j \neq i}} \tag{2.22}$$

The second equality is possible because $g(x)$, the free energy of the crystal at its equilibrium volume, does not depend on elastic strains. So Eq. (2.18) and Eq. (2.19) are summarized as

$$\left(\frac{\partial \tilde{g}_{coex}}{\partial \tilde{\varepsilon}_i} \right)_{x^{\alpha}, x^{\beta}, \tilde{\varepsilon}_{j \neq i}} = \phi^{\alpha} \left(\frac{\partial \tilde{g}_{\alpha}}{\partial \tilde{\varepsilon}_i} \right)_{x_{\alpha}, \tilde{\varepsilon}_{j \neq i}} + \phi^{\beta} \left(\frac{\partial \tilde{g}_{\beta}}{\partial \tilde{\varepsilon}_i} \right)_{x_{\beta}, \tilde{\varepsilon}_{j \neq i}} = 0 \tag{2.23}$$

where implicitly the bulk concentration x is held constant during differentiation. Eq. (2.23) means that the normalized free energy of the two-phase crystallite at the bulk concentration x is minimum with respect to variations in the lateral dimensions in the 2- and 3- directions of the crystallite. The corresponding matrix of second derivatives $(\partial^2 \tilde{g}_{coex} / \partial \tilde{\varepsilon}_i \partial \tilde{\varepsilon}_j)$ is positive definite because the strain energy densities are convex by construction. Hence the extrema are minima.

Since the elastic moduli and lattice parameters depend on chemical concentration, the equations of mechanical and chemical equilibrium are coupled. Consequently, Eq. (2.16)-(2.19) are to be solved simultaneously.

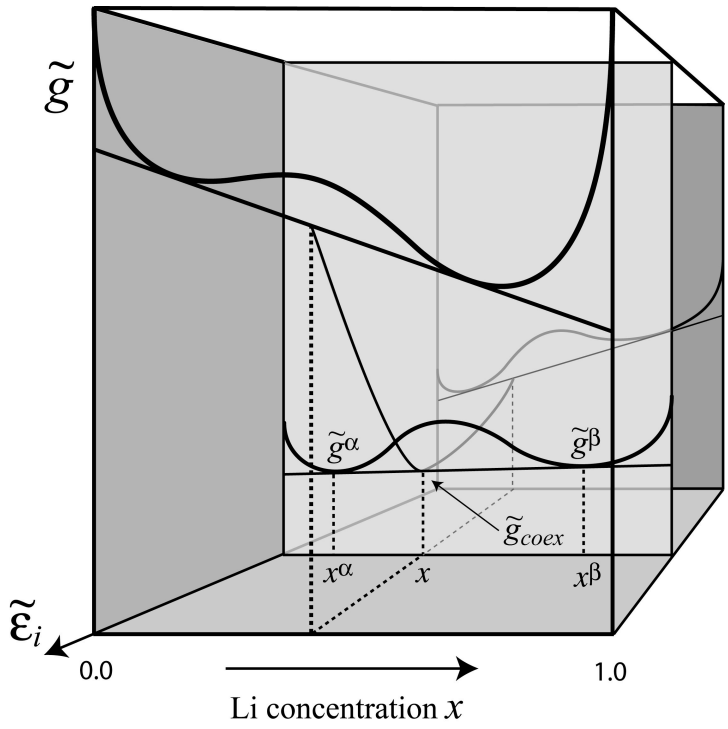

Figure 2.2. Graphical construction of three dimensional common tangent method to find equilibrium strain and concentration in each phase

The general idea of finding global minimum of free energy using common tangent method is illustrated in Fig. 2.2. Once implicitly fixing total concentration *x*, then fixing $\tilde{\varepsilon}_2$ and $\tilde{\varepsilon}_3$, concentrations in two phases are determined. $\tilde{g}_{coex}$ lies on the common tangent at the total concentration, *x*. Then mechanical equilibrium is determined by the minimum of $\tilde{g}_{coex}$ with respect to $\tilde{\varepsilon}_2$ and $\tilde{\varepsilon}_3$.

2. 2. Application to Li_xFePO_4

For Li_xFePO_4, we add some terms to a regular solution model, because behavior of Li_xFePO_4 deviates from a regular solution model due to its eutectoid decomposition as it cools down from solid solution at high temperature. As it cools down, it decomposes to two-phase through a eutectoid reaction with a eutectoid composition at x=0.6. To model free energy more accurately, we used an empirical free energy expression commonly used in calculation of phase diagrams (CALPHAD) descriptions of experimental thermodynamic data, relying on Redlich-Kister polynomial expression [14].

$$g(x) = g_o \cdot (1-x) + g_1 \cdot x + x(1-x)\sum_{n=0}^{m} L_n (1-2x)^n + 2RT\{x\ln x + (1-x)\ln(1-x)\} \tag{2.24}$$

g_0 and g_1 are free energies of $FePO_4$ and $LiFePO_4$, respectively. L_n are Redlich-Kister coefficients and we used terms up to n = 5 for our free energy calculation. The factor of 2 in front of the ideal-solution entropy expression arises from the fact that for every Lithium site that can accommodate Li-vacancy disorder, and there is an Fe site that can accommodate localized electron-hole disorder [15]. The Kister coefficients were adjusted to match voltage curve derived from Eq. (2.24) with experimental open cell voltage curve measured by Meethong el al. [16], and also to have two phase coexistence, illustrated in Fig. 2.3. In Fig. 2.3, no coherency strain energy term is considered.

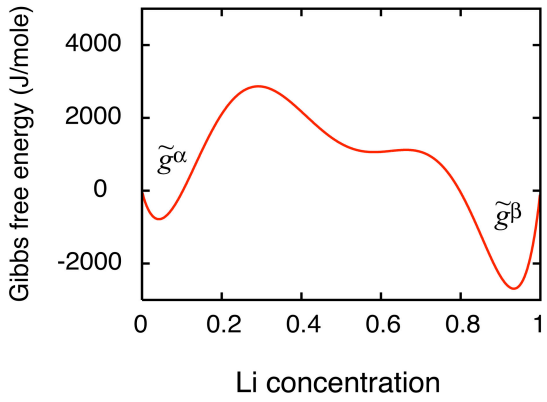

Figure 2.3. Free energy curve without considering the strain energy

We make two more assumptions for Lithium iron phosphate. First, we assume that elastic moduli are independent of Lithium ion concentration. Secondly, we simplify that swelling strain is linearly proportional to concentration following Vegard's law as below, which says that the lattice parameters dependent on Lithium concentration [17].

$$\varepsilon_i^{0\alpha}\left(x^{\alpha}\right) = \tau_i \cdot x^{\alpha} \quad \text{and} \quad \varepsilon_i^{0\beta}\left(x^{\beta}\right) = \tau_i \cdot x^{\beta} \tag{2.25}$$

where i=2, 3.

In Eq. (2.25), τ_i has the same value in both α- and β-phases: τ_2 = 0.036 and τ_3 = -0.186. The values are based on the experimentally measured difference in lattice parameters between and in the 2- and 3-directions [7]. As a quantitative estimate of realistic elastic moduli, we used values predicted from first principles: average values of each c_{ij} for $FePO_4$ and $LiFePO_4$ [13].

property	$FePO_4$	$LiFePO_4$
a [Å]	9.826	10.334
b [Å]	5.794	6.002
c [Å]	4.784	4.695

Table 2.1. Lattice parameters of olivine Li_xFePO_4 from by G. Chen et al. [7]

property	$FePO_4$ GGA+U	$LiFePO_4$ GGA+U
c_{11} [GPa]	175.9	138.9
c_{22} [GPa]	153.6	198.0
c_{33} [GPa]	135.0	173.0
c_{44} [GPa]	38.8	36.8
c_{55} [GPa]	47.5	50.6
c_{66} [GPa]	55.6	47.6
c_{12} [GPa]	29.6	72.8
c_{13} [GPa]	54.0	52.5
c_{23} [GPa]	19.6	45.8
ρ [g/cm^3]	3.51	3.49

Table 2.2. Elastic constants of olivine Li_xPO_4 from first principle calculation by T. Maxisch and G. Ceder [13]

Since total stresses in the 2-direction and 3-direction are zero in Eq. (2.18) and Eq. (2.19), total strain is written as

$$\tilde{\varepsilon}_i = \tau_i x \tag{2.26}$$

Detailed calculation for Eq. (2.26) is shown in the Appendix A. So combining Eq. (2.25) and Eq. (2.26) yields elastic strains in the forms

$$\varepsilon_i^{\alpha} = -\tau_i \cdot \left(x^{\alpha} - x \right) \quad \text{and} \quad \varepsilon_i^{\beta} = -\tau_i \cdot \left(x^{\beta} - x \right) \tag{2.27}$$

By applying Eq. (2.27) to Eq.(2.21) yields

$$\tilde{\mu}^{\alpha}\left(x^{\alpha} \right) = \mu^{\alpha}\left(x^{\alpha} \right) + \Omega\Gamma\left(x^{\alpha} - x \right) \tag{2.28}$$

By integrating Eq. (2.28), we have

$$\tilde{g}^{\alpha}\left(x^{\alpha} \right) = g^{\alpha}\left(x^{\alpha} \right) + \frac{\Omega\Gamma}{2}\left(x^{\alpha} - x \right)^2 \tag{2.29}$$

where

$$\Gamma = \tilde{c}_{22}\tau_2^2 + 2\tilde{c}_{23}\tau_2 \cdot \tau_3 + \tilde{c}_{33}\tau_3^2 \tag{2.30}$$

Eq. (2.29) is applied to two different total concentrations, 0.3 and 0.7 to produce Fig. 2.4, drawn in green curves. The red curves indicate the free energies of homogeneous crystallite having no interface. In Fig. 2.4, the common tangent of green curves in the two-phase coexistent is shown in the black curves. The black curve is always under the red curves in the solubility limits and it means that the coherent crystallites are more plausible to exist than the homogeneous crystallites are.

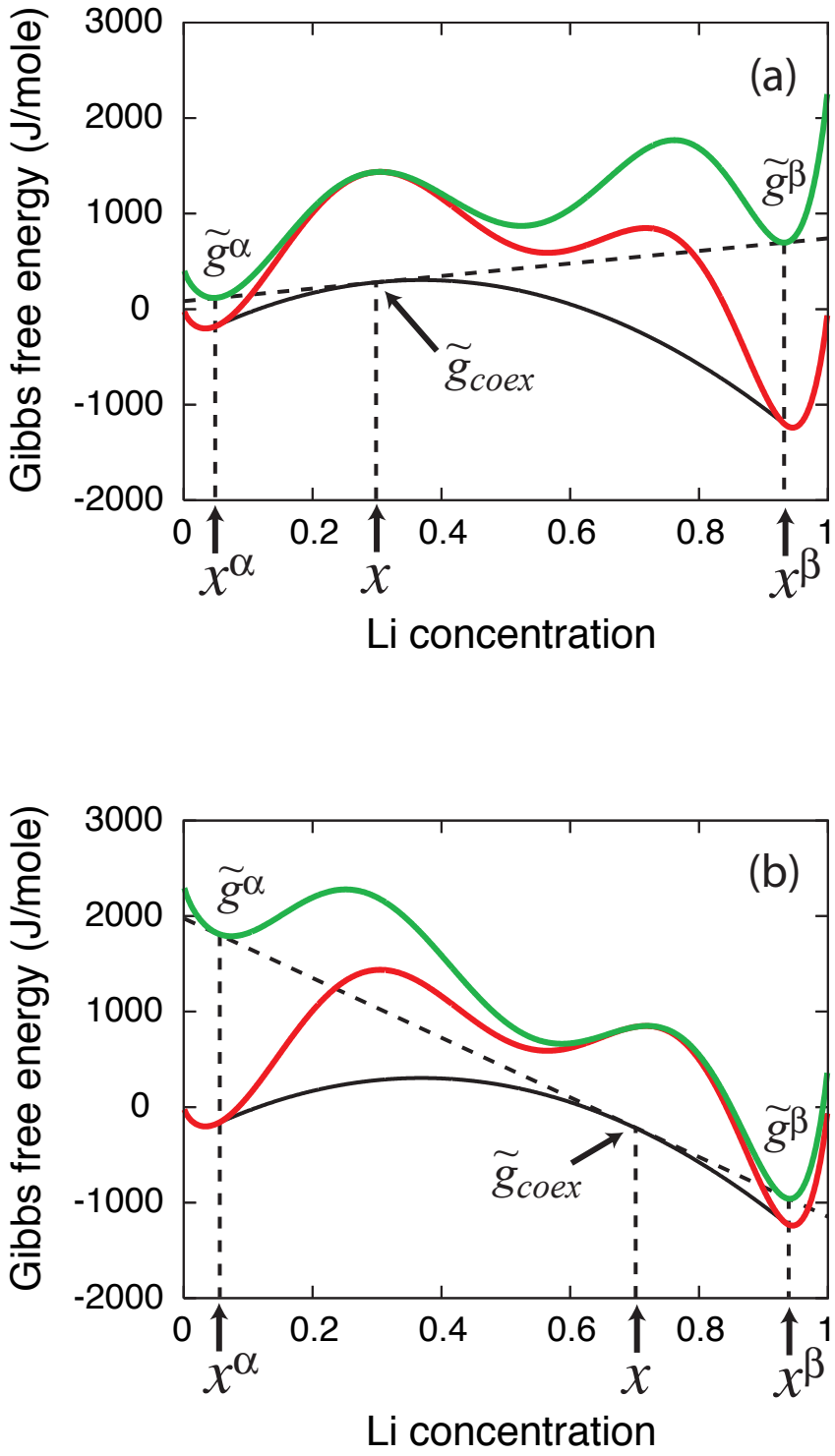

Figure 2.4. Common tangent method for coherent two phase equilibrium, with total concentration (a) x=0.3, (b) x=0.7

2. 3. Effect of coherency strain on two-phase morphologies

Lithium diffusion in Li_xFePO_4 is one-directional along 2-direction or b-direction. Intuitionally two-phase interface is suggested to be perpendicular to the diffusion direction, as the morphology II in Fig 2.5. However, Chen et al. found that the two-phase interface is parallels bc-plane, corresponding to the morphology I illustrated in Fig. 2.5 indicates. They argued that morphology I minimizes the strain energy, an assertion confirmed through our analytic development. Fig. 2.6 illustrates free energies per interstitial site for various possible morphologies in Fig. 2.5. Fig. 2.6 clearly shows that morphology I has a lower free energy than morphology II, consistent with G. Chen et al.'s experimental observations [7].

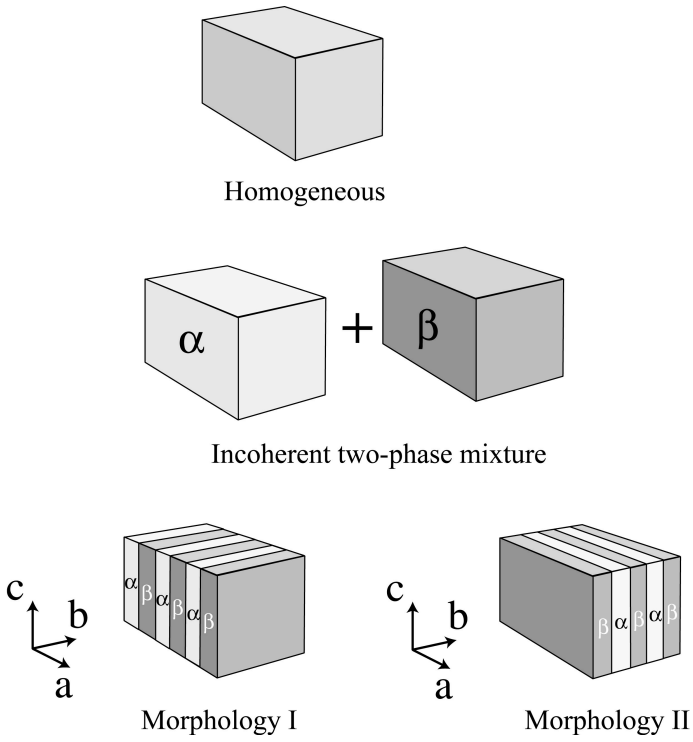

Figure 2.5. Various possible morphologies. At low temperature, morphology I is preferred

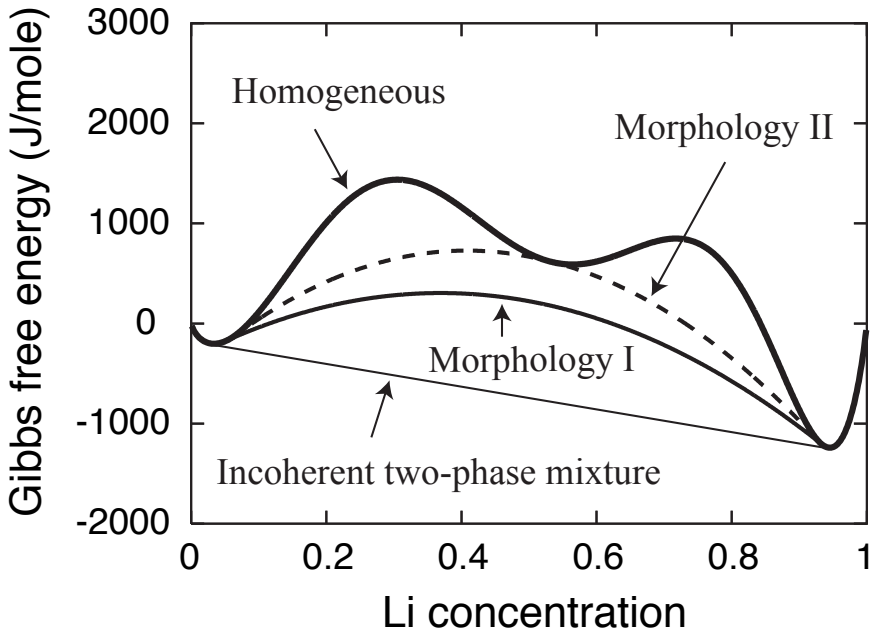

Figure 2.6. Free energies for two-phase coexistence for the various morphologies in Figure 2.5

2. 4. Coherency Strain and Voltage

While the effect of coherency strains is small on each phase concentration, its influence on voltage curve is relatively bigger. Without coherency strain, voltage is constant within a two-phase region as illustrated in Fig. 2.7 as a dashed line. Voltage of Fig. 2.7 is only valid for individual crystallites when the concentration is controlled externally.

The intrinsic voltage is related to Lithium chemical potential of the cathode material crystallite while chemical potential of anode material is constant. F is Faraday's constant in Eq. (2.31).

$$V(x) = -\left(\mu_{Li}^{cathode} - \mu_{Li}^{anode}\right)/eF \tag{2.31}$$

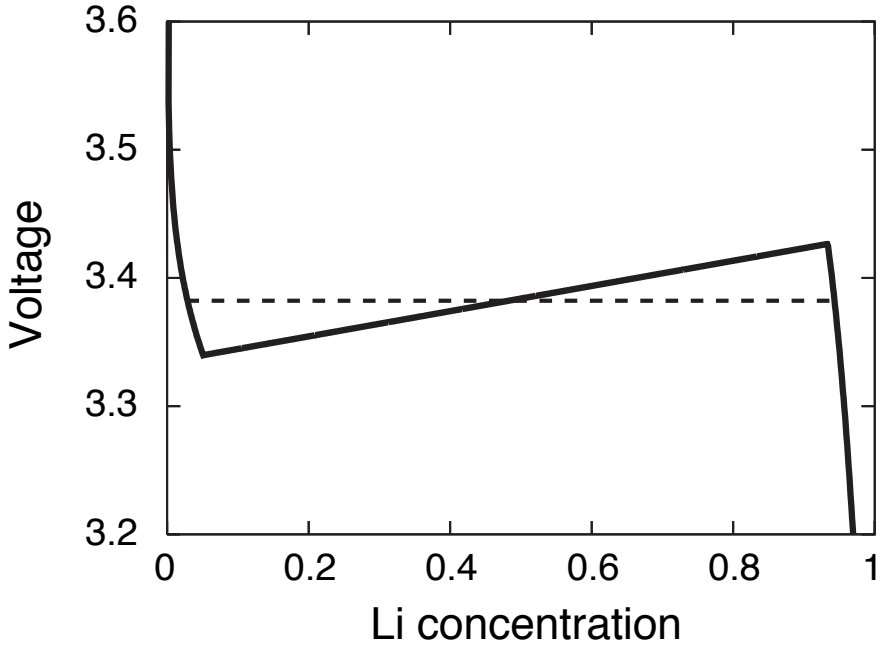

Figure 2.7. Voltage curve for a single crystallite, when controlling total concentration

When the total concentration is controlled externally, voltage increases linearly inside two-phase region due to coherency. Assumptions applied are that elastic moduli are constant and strains follow Vegard's law.

This phenomenon is unlikely to be observed with electrodes consisting of many crystallites, since Lithium ions would redistributed among crystallites. So some crystallites are only in Li-poor phase and some of them are only in Li-rich phase. This is identical with incoherent case. However, during the exchange of Lithium ions, some crystallites are in coherency two-phase equilibrium temporarily. Although, eventually all the crystallites are in single phases, either Li-poor or Li-rich phases.

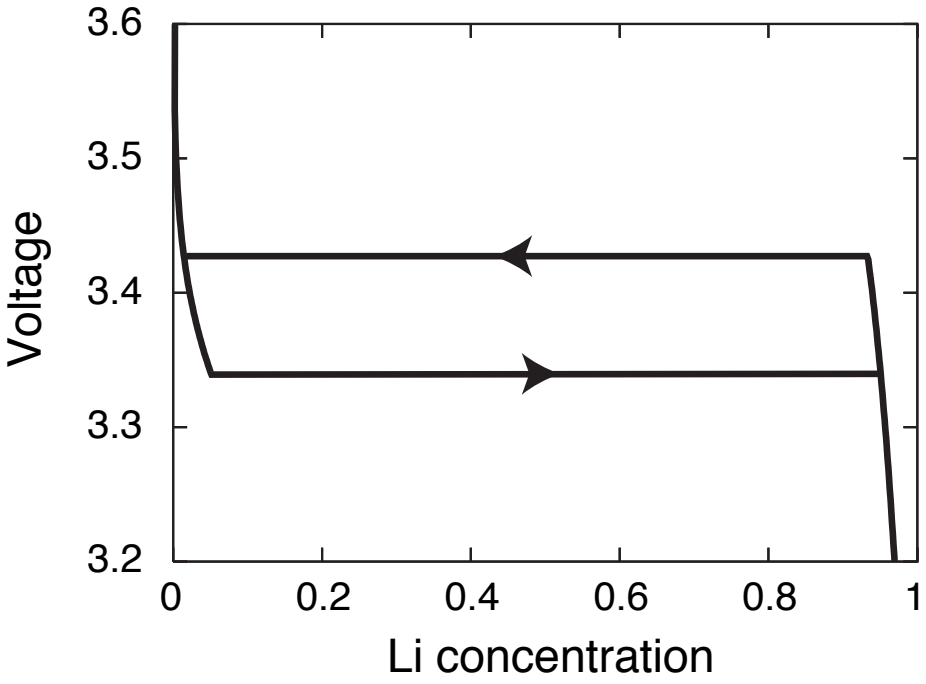

Figure 2.8. Voltage curve showing the role of coherency strain, when controlling voltage

When controlling voltage, which can be done by imposing a constant Lithium chemical potential, we measure concentration. The result, illustrated in Fig. 2.8(a), shows hysteresis. When discharging the coherent electrode, significantly lower underpotential should be applied to overcome coherency strain energy. Once underpotential reaches, the crystallite transforms to Li-rich phase at the constant external voltage. Similarly charging process needs overpotential to transform the crystallite to Li-poor phase. To summarize, coherency strains lead to energy loss to overcome strain energy that is released in an irreversible manners such as sound waves, crack, and dislocation.

2. 5. Periodicity and Error in Analytic Calculation

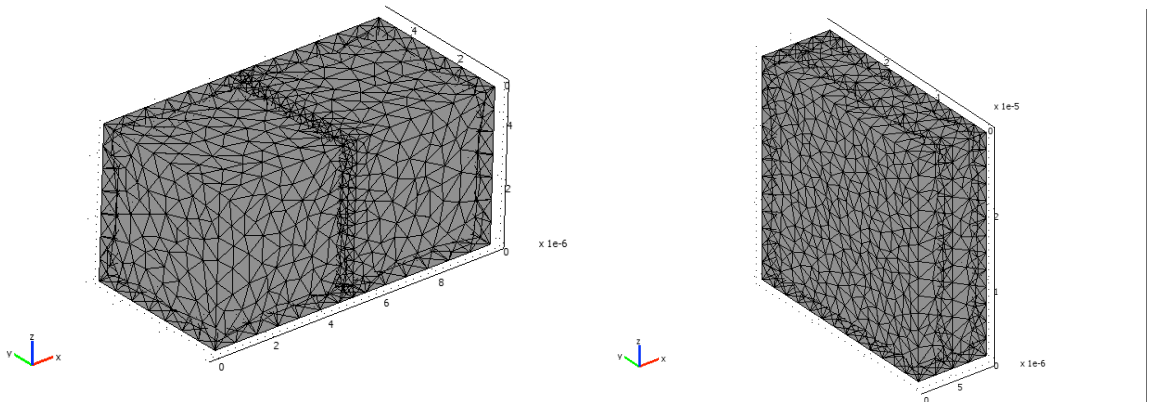

Figure 2.9. Two types of mesh of one periodic cell with ϕ^{β} = 0.5 for FE calculation

In reality, the Li_xFePO_4 crystallite ruffles in the surfaces, while, for our simplified model, only the lattice parameters change as the total concentration changes. Thus our model has smaller degrees of freedom to deform and as a result our analytic strain energies are the upper bounds for real. With periodicity in α and β phases along a-direction, as illustrated in Fig. 2.10, our model depicts a real crystallite better, for the crystallite rumples less in that case. In Fig. 2.10, we confirm that as periodicity increases, relative errors in strain energy between our analytical model and more realistic FE model decrease. For simplicity, we considered a rectangular shaped crystal with same lengths L_2 and L_3 along 2- and 3-directions while changing the length of periodicity λ_1 along first direction. Analytic calculation is based on the result of section 2.2, while the COMSOL software was used for FE calculations. In Fig. 2.10, the crystallite is free to deform in the first direction that is perpendicular to the phase interfaces. In FE

computation, the free boundary condition along the 1-direction is substituted by modifying the displacement along first direction until the stress in the 1-direction, σ_1 reaches zero. The calculation was conducted with three different phase fractions: 0.01, 0.05, and 0.50. As illustrated in Fig. 2.10, the result shows that smaller fraction insertions of different phase cause smaller relative errors between analytic and FE calculation. The result meets the intuition because smaller fraction of dissimilar phase insertions make the crystallite almost homogeneous. The discrepancy of FE and analytic calculations for phase fraction 0.99 will have similar value to that for phase fraction 0.01. Similarly, so will be the difference with phase fraction 0.05 to that with phase fraction 0.95. We expect the maximum discrepancy will happen near the phase fraction 0.50.

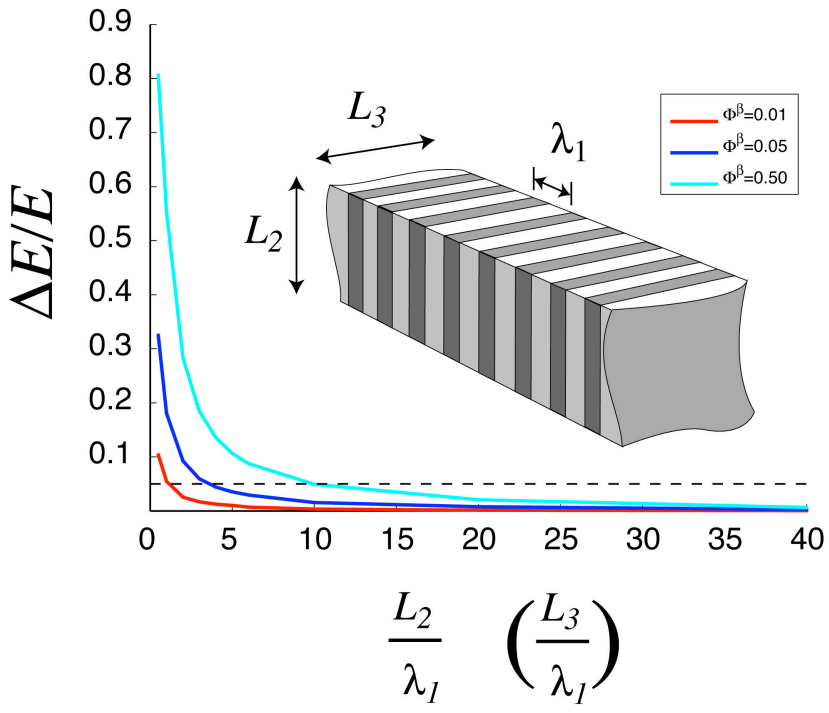

Figure 2.10. Relative error of analytic approximation compared to FE calculation as a dimension of periodicity changes. The dashed line indicates 5% error

2. 6. Ideal Crystallite Shape Based on Quasi-Static Analysis

The coherency strain energy scales with the size of the crystallite and depends on the shape of the crystallite. For macroscopic crystallites, coherency strain energy is too big to overcome by thermal fluctuation and only with a huge overpotential in the voltage can two-phase coexistence be achieved. One way to reduce required overpotential per volume of a macroscopic crystallite is to change shape of the crystallite to reduce coherency strain. Through finite element analysis, we found that needle shape crystallites have the least coherency strain energy densities, as illustrated in Fig. 2.11. So minimum overpotential in the voltage is needed for two-phase coexistence in the needle shape crystallites. Since the needle shape will have the least area of two-phase interfaces per volume of a crystallite and hence the least coherency strain energy, the result meets intuitions. A minimization of coherency strain also reduces possibility of mechanical damages. Large localized stress during two-phase coexistence can results in irreversible dislocations and cracks. These crystalline defects hamper the passage of the interfaces during phase transformations and result in overall particle degradation. As the crystallites approach the nanoscale, the total coherency strain energy becomes small too. At the nanoscale, the coherency strain energy may become comparable to thermal energy and could be overcome by thermal fluctuations. So less of an overpotential is needed to initiate phase transformation.

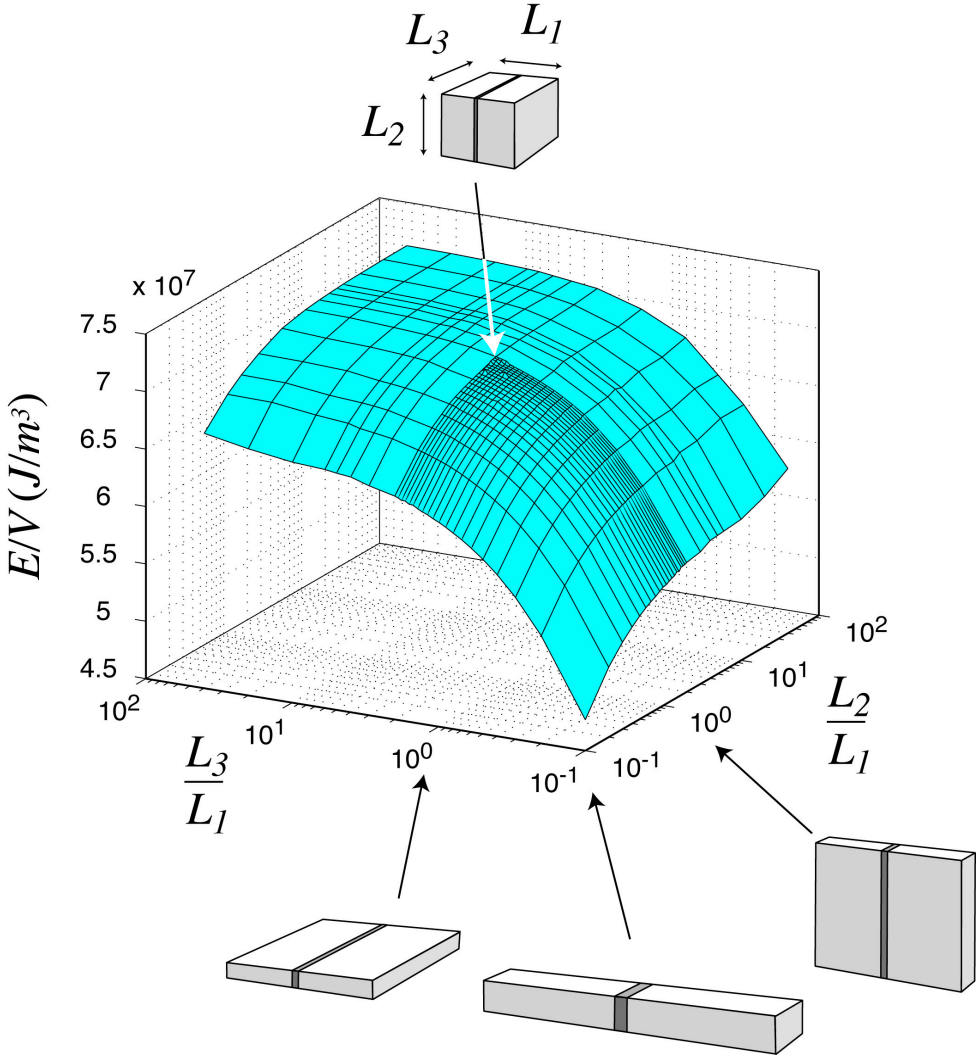

Figure 2.11. Coherency strain energy density as function of crystallite dimensions when α–phase is enclosed by β-phase

CHAPTER III

Time dependent FE analysis of electrode materials

In this chapter, a time dependent analysis scheme for the Lithium (de)intercalation processes of Li-ion battery electrodes will be conducted. There exist moving interfaces between two coherent phases. Right behind the moving interface, the newly phase-transformed part experiences infinitesimal structural changes from concentration transition. We will formulate the diffusion process and stress equilibrium for the Lithium (de)intercalation process both rigorously and numerically. Tracking of the moving interfaces will be conducted with the Level Set Method. The coupled physics are illustrated in Figure (3.1) for a special case of Li_xFePO_4 with one-dimensional diffusion along the b-axis.

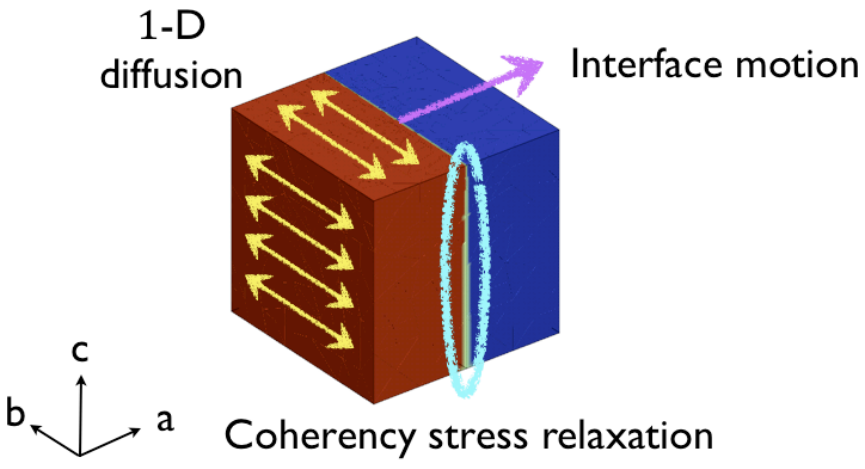

Figure 3.1. Time dependent coupled physics for Li_xFePO_4

3. 1. Mathematical Formulation

3. 1. 1. Transport problem

We use the mass balance equation with a sharp interface for the diffusion problem. At the interface, the concentration changes discontinuously. The strong form of transport problem is

$$\frac{\partial x^{\xi}}{\partial t} = -\nabla \cdot j^{\xi}$$
$$j^{\xi} = -D^{\xi} \nabla x^{\xi} \tag{3.1}$$

where $\xi = \alpha$ and β. Eq. (3.1) is second Fick's law.

In Eq. (3.1), x^{ξ}, D^{ξ}, and j^{ξ} are the concentration of each phase, diffusivity, and flux of each phase respectively. The anisotropic diffusion is possible by setting D^{ξ} as

$$D^{\xi} = \begin{bmatrix} D_1 & 0 & 0 \\ 0 & D_2 & 0 \\ 0 & 0 & D_2 \end{bmatrix} \tag{3.2}$$

where the a-direction is perpendicular to the interface for the case of Li_xFePO_4.

For Li_xFePO_4, the diffusion is confined to one-dimensional channels parallel to the a-direction [18]. Here two dimensional diffusivity for Li_xFePO_4 is considered to calculate the velocity of the propagating phase interface: $D_1 \gg D_2$, $D_3 = 0$.

The weak Form of Eq. (3.1) is

$$\int_{\Omega^\alpha \cup \Omega^\beta} \left(w \frac{\partial x}{\partial t} + w \nabla \cdot j \right) dV = 0 \tag{3.3}$$

where *w* is a weighting function.

By applying the divergent theorem to Eq. (3.3) and then enumerating all the boundaries including the interface flux in the phase-interface Γ between Li-poor α–phase and Li-rich β-phase, we have

$$\begin{aligned} &\int_{\Omega^\alpha \cup \Omega^\beta} w \frac{\partial x}{\partial t} dV - \int_{\Omega^\alpha \cup \Omega^\beta} \nabla w \cdot j dV + \int_{\partial \Omega^\alpha \setminus \Gamma} w j^\alpha \cdot n dV \\ &+ \int_{\partial \Omega^\beta \setminus \Gamma} w j^\beta \cdot n dS + \int_{\Gamma^\beta} w j^\beta \cdot n dS + \int_{\Gamma^\alpha} w j^\alpha \cdot (-n) dS = 0 \end{aligned} \tag{3.4}$$

where the normal vector at the interface is illustrated in Fig. 3.1.

With a discontinuity bracket defined below, we define flux jump at the interface Γ.

$$[\![j \cdot n]\!] = (j^\beta - j^\alpha) \cdot n \tag{3.5}$$

With Eq. (3.4) and (3.5), the weak form of the transport problem becomes

$$\int_{\Omega^\alpha \cup \Omega^\beta} w \frac{\partial x}{\partial t} dV - \int_{\Omega^\alpha \cup \Omega^\beta} \nabla w \cdot j dV + \int_{\partial \Omega^\alpha \setminus \Gamma} w j^\alpha \cdot n dV + \int_{\partial \Omega^\beta \setminus \Gamma} w j^\beta \cdot n dS + \int_{\Gamma^\beta} w [\![j \cdot n]\!] dS = 0 \tag{3.6}$$

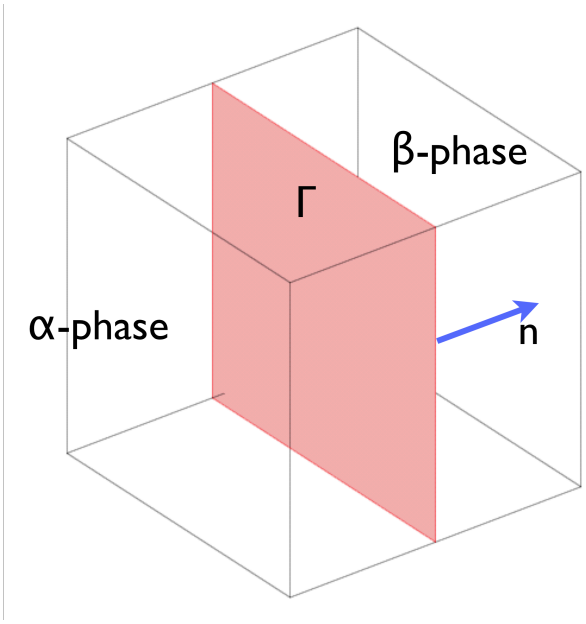

Figure 3.2. Definition of normal vector, *n*, at the interface *Γ*

When seen from a moving frame Γ in Figure 3.3, conservation of mass can be expressed as

$$j^\alpha \cdot n - c^\alpha v \cdot n = j^\beta \cdot n - c^\beta v \cdot n \tag{3.7}$$

where v is the velocity of the interface.

So the velocity of interface can be calculated as

$$v \cdot n = \frac{(j^{\alpha} - j^{\beta}) \cdot n}{x - x} = \frac{[\![j \cdot n]\!]}{[\![x]\!]} \tag{3.8}$$

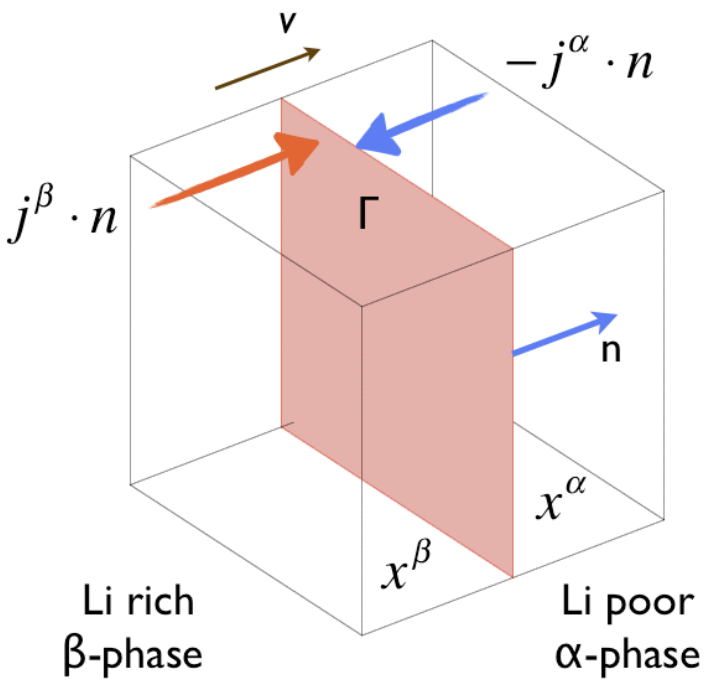

Figure 3.3. Mass balance at the interface *Γ*

Both essential and natural boundary conditions are possible to simulate the transport problem correctly. First, an essential boundary condition on the surface with active reaction and natural boundary condition for inactive rest can be applied.

$$\begin{gathered} x = x^{\alpha} \text{ on } \partial\Omega_{\alpha} \\ \text{no flux on } \partial\Omega_{\beta} \end{gathered} \tag{3.9}$$

Alternatively, a natural boundary condition, Eq. (3.10) can be applied. For Li_xFePO_4, the only two non-zero components are g_2^α and g_2^β, because of the one-dimensional anisotropic diffusion property of the material.

$$j = \begin{pmatrix} g_1^\alpha \\ g_2^\alpha \\ g_3^\alpha \end{pmatrix} \text{ on } \partial\Omega_\alpha$$
$$j = \begin{pmatrix} g_1^\beta \\ g_2^\beta \\ g_3^\beta \end{pmatrix} \text{ on } \partial\Omega_\beta \tag{3.10}$$

3. 1. 2. Mechanical Problem

Generally stress relaxation happens faster than the diffusion process in the Li-ion battery materials. Hence we adopt quasi-static stress equilibrium in the reference configuration with a natural boundary condition for all outer boundaries.

$$\nabla \cdot P = 0 \tag{3.11}$$

$$T = n \cdot P = 0 \tag{3.12}$$

where P is the first Piola-Kirchhoff stress tensor and T is a traction force on the surface.

The weak form is

$$\int_{\Omega^\alpha \cup \Omega^\beta} P \cdot \nabla \vec{w}\, dV - \int_{\partial\Omega^\alpha \cup \partial\Omega^\beta} \vec{w} T\, dS = 0 \quad \text{where } \vec{w} \text{ is the weighting funciton} \qquad (3.13)$$

From the Neumann condition, Eq. (3.12), Eq.(3.13) is simplified to

$$\int_{\Omega^\alpha \cup \Omega^\beta} P \cdot \nabla \vec{w}\, dV = 0 \qquad (3.14)$$

We calculate *P* from the following strain energy function.

$$\begin{aligned} W &= \frac{1}{2} E_{ij} C_{ijkl} E_{kl} \\ &= \frac{1}{2}(E_{11}^2 C_{1111} + E_{22}^2 C_{2222} + E_{33}^2 C_{3333} \\ &\quad + 2E_{11}E_{22}C_{1122} + 2E_{11}E_{33}C_{1133} + 2E_{22}E_{33}C_{2233} \\ &\quad + 4E_{12}^2 C_{1212} + 4E_{13}^2 C_{1313} + 4E_{23}^2 C_{2323}) \\ &= \frac{1}{2}(E_{11}^2 C_{11} + E_{22}^2 C_{22} + E_{33}^2 C_{33} \\ &\quad + 2E_{11}E_{22}C_{12} + 2E_{11}E_{33}C_{13} + 2E_{22}E_{33}C_{23} \\ &\quad + 4E_{12}^2 C_{66} + 4E_{13}^2 C_{55} + 4E_{23}^2 C_{44}) \end{aligned} \qquad (3.14)$$

Through partial differentiation of Eq. (3.14) with the deformation gradient tensor *F*, we get

$$P = \frac{\partial W}{\partial F} = \frac{\partial W}{\partial E}\frac{\partial E}{\partial F} = F\frac{\partial W}{\partial E} = F(C:E) \tag{3.15}$$

The components of *P* are shown in Eq. (3.17)

$$P_{ik} = F_{ij}(C_{jklm}E_{lm}) \tag{3.16}$$

$$\begin{aligned}
P_{11} &= F_{11}C_{11}E_{11} + F_{12}(C_{12}+C_{66})E_{21} + F_{13}(C_{13}+C_{55})E_{31}\\
P_{22} &= F_{21}(C_{12}+C_{66})E_{12} + F_{22}C_{22}E_{22} + F_{23}(C_{23}+C_{44})E_{32}\\
P_{33} &= F_{31}(C_{13}+C_{55})E_{13} + F_{32}(C_{23}+C_{44})E_{23} + F_{33}C_{33}E_{33}\\
P_{23} &= F_{21}(C_{13}+C_{55})E_{13} + F_{22}(C_{23}+C_{44})E_{23} + F_{23}C_{33}E_{23}\\
P_{13} &= F_{11}(C_{13}+C_{55})E_{13} + F_{12}(C_{23}+C_{44})E_{23} + F_{13}C_{33}E_{33}\\
P_{12} &= F_{11}(C_{12}+C_{66})E_{12} + F_{12}C_{22}E_{22} + F_{13}(C_{23}+C_{44})E_{32}
\end{aligned} \tag{3.17}$$

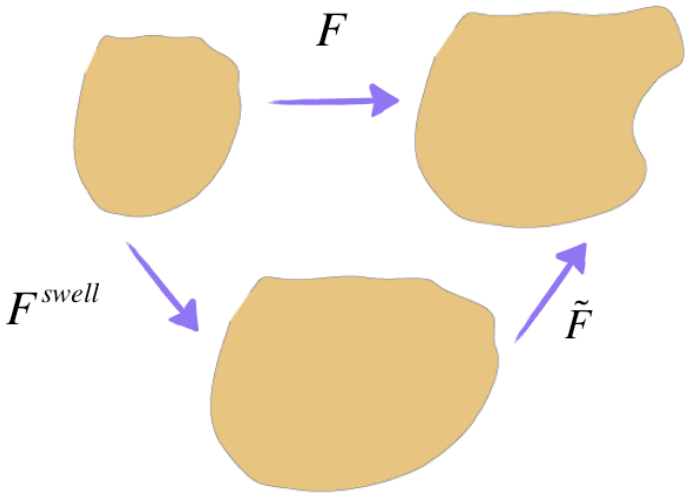

Figure 3.4. Decomposition of the deformation gradient tensor

As the concentration of the Lithium changes, swelling happens in the crystallite. I assume that the changes in lattice parameters follow Vegard's law: the changes in lattice parameters are linearly dependent on the Lithium concentration, *x*. The anisotropic expansion is handled by multiplying swelling term to deformation gradient. Since any motions can be decomposed to pure swelling due to the chemical composition change and typical deformation tensor, the deformation gradient tensor can be decomposed to

$$F = F^{swell}\tilde{F} \tag{3.18}$$

where deformation gradient tensor from chemical composition is defined as

$$F^{swell} = \frac{(a_1 - a_0)x^{\xi}}{a_0}\vec{e}_1 \otimes \vec{e}_1 + \frac{(b_1 - b_0)x^{\xi}}{b_0}\vec{e}_2 \otimes \vec{e}_2 + \frac{(c_1 - c_0)x^{\xi}}{c_0}\vec{e}_3 \otimes \vec{e}_3 \tag{3.19}$$

where a_0, b_0, and c_0 are lattice parameters of fully delithiated phase and a_1, b_1, and c_1 are those of fully lithiated phase. This decomposition process matches Eq.(2.3) in the Chapter II.

3. 1. 3. Two-Phase Interface Tracking by Level Set Method

The brief explanation of Level set method in this section is excerpted from chapter two of James Sethian's book [8]. Stanley Osher and James Sethian developed Level set method (LSM) to track interfaces and boundaries. LSM calculation is carried out with fixed Cartesian grid (Eulerian perspective) and can be applied to complex topology changes such as hole developing and surface splitting.

Let the dimension of domain Ω be N. Then LSM embeds propagating hypersurface Γ of (N-1)-dimension as the zero level set of a higher dimensional function ϕ.

The function ϕ is called signed function. Initial values of ϕ are the distance from the hypersurface Γ, where d is the distance from the hypersurface.

$$\phi(x, t = 0) = \pm d \tag{3.20}$$

The initial hypersurface is defined as

$$\Gamma(t = 0) = \left[x \,||\, \phi(x, t = 0) = 0 \right] \tag{3.21}$$

In Eq. (3.21), plus (minus) sign indicates that the corresponding point x is outside (inside) of the initial closed hypersuface Γ. The requirement is that as time passes, the evolving zero level set always matches the propagating hypersuface.

$$\phi(x(t), t) = 0 \tag{3.22}$$

By applying the chain rule to Eq. (3.22), we get

$$\frac{\partial \phi}{\partial t} + \nabla \phi \cdot x'(t) = 0$$

$$\frac{\partial \phi}{\partial t} + \nabla \phi \cdot v(t) = 0 \tag{3.23}$$

With the velocity of interface, *v*, defined in Eq. (3.8), an advection equation is set to be solved. The boundary condition for Eq. (3.23) is

$$\phi = 0 \text{ or } \hat{n}_{wall} \cdot \nabla \phi = 0 \text{ on } \partial\Omega, t = [0, T]$$

$$\text{where } \hat{n}_{wall} \text{ is the normal vector at the walls} \tag{3.24}$$

So the weak form of Eq. (3.24)

$$\int_{\Omega} w \frac{\partial \phi}{\partial t} dV + \int_{\Omega} w(v \cdot \nabla \phi) dV = 0 \tag{3.25}$$

is solved and the zero contour of solution indicates the location of interface.

We use a modified version of LSM by E. Olsson et al. [19] The modified version differs in the initial condition from the original one and has enhanced mass conservation property. Also, reinitialization of initial condition, which is generally required for correct LSM calculation, is not necessary with the Olsson's LSM in Eq (3.25) because of its conservative property.

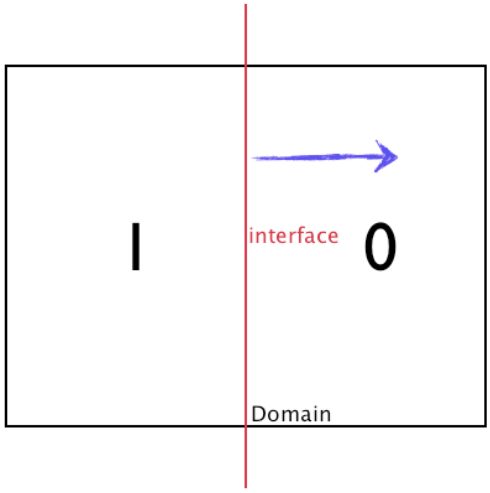

Figure 3.5. Initial condition of E. Olsson's LSM

$$H_{sm}(\phi)=\begin{cases}0, & \phi\le-\delta\\ \dfrac{1}{2}+\dfrac{\phi}{2\delta}+\dfrac{1}{2\pi}\sin\left(\dfrac{\pi\phi}{\delta}\right), & -\delta\le\phi\le\delta\\ 1, & \phi>\delta\end{cases} \tag{3.26}$$

When the advection term is dominating, numerical instability can be alleviated in a consistent manner by adding residual based terms over the element interiors to the Galerkin weak form. There are several ways to stabilize the equation, *e.g.*, Streamlined Upwind Petrov-Galerkin (SUPG) and Galerkin Least Squares method (GLS) [20, 21]. E. Olsson's version has a little complex spacial stabilizing scheme to guarantee mass conservation especially for fluids problems. Instead of the complex stabilizing scheme, we adopt SUPG for the LSM. By adding SUPG term to Eq. (3.24), we get

$$\int_{\Omega} w\phi_t \, dV + \int_{\Omega} w(v \cdot \nabla\phi) dV + \underbrace{\int_{\Omega} \tau(\frac{\partial w}{\partial t} + v \cdot \nabla\phi)(\phi_t + v \cdot \nabla\phi - f) dV}_{SUPG} = 0 \qquad (3.26)$$

For time stepping, forward Euler method is applied to both transport problem and interface tracking LSM.

3. 2. Staggered Algorithm

Now that we have defined all three physics in the weak form, we can solve the whole problem. Solving the coupled problem simultaneously is ideal to a get correct solution. If we want to reduce the computational cost, we can adopt the staggered algorithm, which solve one equation while fixing other variables, then solve another equation in a similar manner.

CHAPTER IV

Conclusion and Future Work

4. 1. Conclusion

A single crystallite of many electrodes for Li-ion batteries undergoes two-phase coexistent states during (dis)charge, since the crystallite of electrodes often have lower free energies when two phase coexist. When two phases coexist, very sharp or somewhat diffused interfaces between the two-phase portions have been observed in many electron microscopy studies. The different lattice parameters for each phase portion result in coherency strain at the phase interface. This coherency strain affects chemical potential and total free energy. Reversely, changed thermodynamic potentials vary solubility limits of Lithium, voltage profile, and phase stability. We suggested a way to model the coupled Lithium (de)intercalation kinetics both analytically and numerically.

In the quasi-static analysis, we derived mechanical and chemical equilibrium criteria and applied them to olivine Li_xFePO_4 ($0 \leq x \leq 1$) prism-shape crystallite. We added coherency strain energy term to the free energy and found four equilibrium conditions: two chemical and two mechanical equilibrium criteria. Two chemical equilibrium criteria correspond to the well known common tangent method with modified chemical potential and modified total free energy by added coherency strain

energy. The rest two mechanical equilibrium means that the average stresses along two directions equals zero, which parallel the phase interface.

When applying the criteria to olivine Li_xFePO_4 crystallite, further assumptions were made: (i) the elastic moduli are independent of the Lithium concentration and (ii) the lattice parameters are linearly proportional to the Lithium concentration. We check the effect of coherency strain on the voltage profile. Using the Lithium chemical potential of Li_xFePO_4 crystallite, the effect of coherency strains on overpotential and underpotential to initiate evolution of coherency crystallite was shown. For olivine Li_xFePO_4 crystallite, by adding the coherency strain energy term to the total free energy, we confirmed that the total energy is minimized when the phase interface parallels the bc-plane, although the Lithium ions diffuse along the b-axis of the crystallite.

Since actual crystallites ruffle in the surface, the free energy of the developed analytic solution is always higher than the real value. One way to make the analytic solution more accurate is increasing periodicity to alleviate the ruffles in the surface can be alleviated. By comparing analytic solution with more realistic finite element calculation, we confirmed that as periodicity increases, relative errors in strain energy between our analytical model and more realistic finite element model decrease. Also, the comparison confirmed the intuition that a smaller fraction of dissimilar phase insertion leads to smaller surface ruffles. Because, with small fraction of alien phase, the crystallite is more similar to the one in a homogenous state, the ideal analytic calculations becomes closer to the more accurate FE calculations. Through the FE analysis, we found that minimal coherency strain energy density corresponds to needle-shape crystallite for the quasi-static case.

In time dependent analysis, fully coupled general scheme for 3 physics is shown: diffusion, coherent stress relaxation, and the two-phase interface evolution. First, the diffusion equation dealt the Lithium ion diffusion in the host. Second, the mechanics equation for the coherent stress relaxation is slight modification of quasi-static analysis. Finally, the evolving two-phase interface was handled with the Level Set Method. We adopted E. Olsson's modified version of LSM and changed the spacial stabilizing scheme of it with SUPG. We hope that fully coupled time dependent three-dimensional numerical simulation of the electrode materials will inspire readers about new designs of these materials.

For the application to Li_xFePO_4, the quantitative as well as qualitative predictions of our development are sensitive to the behavior of the free energy of the homogeneous phase inside the incoherent two-phase region. This portion of the free energy of Li_xFePO_4 is currently unknown and very difficult to be measured experimentally. The effect of coherency strain on the composition of the coexisting phases, x^{α} and x^{β}, will be more significant than predicted here if the difference between the homogeneous free energy inside the two-phase region and the common tangent , Δg, is smaller than one in the free energy model of Li_xFePO_4 used in the Chapter II. Also, two-phase coexistence could be completely suppressed within individual crystallites at room temperature if the maximum value of Δg inside the two-phase region is less than the coherency strain energy penalty of two-phase coexistence.

4. 2. Future Work

Implementation of the time-dependent scheme to actual electrode materials will confirm the validness of the derivation in Chapter III. The sharp interface with discontinuously changing concentration generally leads to oscillation. To accurately model the discontinuously changing concentration, I recommend to adopt the Discontinuous Galerkin (DG) method [22] or the enhanced strain approach [23]. Both methods are stable when there is jumps in the field variables: strains and concentration.

APPENDICES

APPENDIX A

A.1. Plane Stress Elastic Moduli Derivation

From the plane stress assumption, we set the stress along first direction is zero.

$$\sigma_1 = c_{11}\varepsilon_1 + c_{12}\varepsilon_2 + c_{13}\varepsilon_3 = 0 \tag{A.1}$$

From Eq. (A.1), we get

$$\varepsilon_1 = -\frac{1}{c_{11}}(c_{12}\varepsilon_2 + c_{13}\varepsilon_3) \tag{A.2}$$

The stresses in the 2nd and 3rd direction are

$$\begin{aligned} \sigma_2 &= c_{21}\varepsilon_1 + c_{22}\varepsilon_2 + c_{23}\varepsilon_3 \\ \sigma_3 &= c_{31}\varepsilon_1 + c_{32}\varepsilon_2 + c_{33}\varepsilon_3 \end{aligned} \tag{A.3}$$

By eliminating ε_1 in Eq. (A.3), we get

$$\sigma_2 = (c_{22} - \frac{c_{12}c_{12}}{c_{11}})\varepsilon_2 + (c_{23} - \frac{c_{13}c_{13}}{c_{11}})\varepsilon_3$$
$$\sigma_3 = (c_{23} - \frac{c_{12}c_{12}}{c_{11}})\varepsilon_2 + (c_{33} - \frac{c_{13}c_{13}}{c_{11}})\varepsilon_3 \quad \text{(A.4)}$$

Now, by defining the plane stress moduli as below,

$$\tilde{c}_{ij} = (c_{ij} - \frac{c_{1i}c_{1j}}{c_{11}}) \quad \text{(2.7)}$$

where *i, j* =2,3.

we can express the stresses in the second and third directions as

$$\sigma_2 = \tilde{c}_{22}\varepsilon_2 + \tilde{c}_{23}\varepsilon_3$$
$$\sigma_3 = \tilde{c}_{23}\varepsilon_2 + \tilde{c}_{33}\varepsilon_3 \quad \text{(A.5)}$$

A. 2. Coherent Two-Phase Equilibrium Criteria Derivation

The total Gibbs free energy is shown in Eq. (2.5).

$$G = \phi^{\alpha} M \cdot g^{\alpha}\left(x^{\alpha}\right) + \phi^{\beta} M \cdot g^{\beta}\left(x^{\beta}\right) + E^{strain} \quad \text{(2.5)}$$

where M as total number of Li interstitial sites within the crystallite.

In Eq. (2.5), strain energy is

$$E^{strain} = \frac{1}{2}\int_{V_0}\left[\sigma_2\varepsilon_2 + \sigma_3\varepsilon_3\right]dV_0 = \frac{1}{2}\int_{V_0}\left[\tilde{c}_{22}\left(\varepsilon_2\right)^2 + 2\tilde{c}_{23}\left(\varepsilon_2\cdot\varepsilon_3\right) + \tilde{c}_{33}\left(\varepsilon_3\right)^2\right]dV_0 \tag{2.6}$$

Assuming that strains in each phase are uniform, elastic energy in Eq. (2.6) is simplified to

$$E^{strain} = V_0\left(\phi^\alpha e^\alpha\left(\varepsilon_2^\alpha,\varepsilon_3^\alpha\right) + \phi^\beta e^\beta\left(\varepsilon_2^\beta,\varepsilon_3^\beta\right)\right) \tag{2.8}$$

where

$$e^\xi\left(\varepsilon_2,\varepsilon_3\right) = \frac{1}{2}\left[\tilde{c}_{22}\left(\varepsilon_2^\xi\right)^2 + 2\tilde{c}_{23}\left(\varepsilon_2^\xi\cdot\varepsilon_3^\xi\right) + \tilde{c}_{33}\left(\varepsilon_3^\xi\right)^2\right] \tag{2.9}$$

In Eq. (2.5), we choose four independent variables:

N^α, ϕ^α, $\tilde{\varepsilon}_2$, and $\tilde{\varepsilon}_3$.

To find equilibrium criteria, we minimize the total free energy with respect to the four chosen variables. First one is

$$\left(\frac{\partial G}{\partial N^\alpha}\right)_{\phi^\alpha,\tilde{\varepsilon}_2,\tilde{\varepsilon}_3} = 0 \tag{2.12}$$

To expand Eq. (2.12)

$$
\begin{aligned}
&\phi^{\alpha} M \frac{\partial x^{\alpha}}{\partial N^{\alpha}} \frac{\partial g^{\alpha}}{\partial x^{\alpha}} + \phi^{\beta} M \frac{\partial x^{\beta}}{\partial N^{\alpha}} \frac{\partial g^{\beta}}{\partial x^{\beta}} \\
&+ \frac{V_0 \phi^{\alpha}}{2} \frac{\partial x^{\alpha}}{\partial N^{\alpha}} \left[\left(\varepsilon_2^{\alpha} \right)^2 \frac{\partial \tilde{c}_{22}^{\alpha}}{\partial x^{\alpha}} + 2(\varepsilon_2^{\alpha} \cdot \varepsilon_3^{\alpha}) \frac{\partial \tilde{c}_{23}^{\alpha}}{\partial x^{\alpha}} + \left(\varepsilon_3^{\alpha} \right)^2 \frac{\partial \tilde{c}_{33}^{\alpha}}{\partial x^{\alpha}} \right] \\
&+ \frac{V_0 \phi^{\beta}}{2} \frac{\partial x^{\beta}}{\partial N^{\alpha}} \left[\left(\varepsilon_2^{\beta} \right)^2 \frac{\partial \tilde{c}_{22}^{\beta}}{\partial x^{\beta}} + 2(\varepsilon_2^{\beta} \cdot \varepsilon_3^{\beta}) \frac{\partial \tilde{c}_{23}^{\beta}}{\partial x^{\beta}} + \left(\varepsilon_3^{\alpha} \right)^2 \frac{\partial \tilde{c}_{33}^{\beta}}{\partial x^{\beta}} \right] \\
&+ V_0 \phi^{\alpha} \frac{\partial x^{\alpha}}{\partial N^{\alpha}} \left[\left(\frac{\partial e^{\alpha}}{\partial \varepsilon_2^{\alpha}} \frac{\partial \varepsilon_2^{\alpha}}{\partial \varepsilon_2^{0\alpha}} \frac{\partial \varepsilon_2^{0\alpha}}{\partial x^{\alpha}} \right) + \left(\frac{\partial e^{\alpha}}{\partial \varepsilon_3^{\alpha}} \frac{\partial \varepsilon_3^{\alpha}}{\partial \varepsilon_3^{0\alpha}} \frac{\partial \varepsilon_3^{0\alpha}}{\partial x^{\alpha}} \right) \right] \\
&+ V_0 \phi^{\beta} \frac{\partial x^{\beta}}{\partial N^{\alpha}} \left[\left(\frac{\partial e^{\beta}}{\partial \varepsilon_2^{\beta}} \frac{\partial \varepsilon_2^{\beta}}{\partial \varepsilon_2^{0\beta}} \frac{\partial \varepsilon_2^{0\beta}}{\partial x^{\beta}} \right) + \left(\frac{\partial e^{\beta}}{\partial \varepsilon_3^{\beta}} \frac{\partial \varepsilon_3^{\beta}}{\partial \varepsilon_3^{0\beta}} \frac{\partial \varepsilon_3^{0\beta}}{\partial x^{\beta}} \right) \right] = 0
\end{aligned}
\tag{A.6}
$$

To simplify Eq. (A.6), we use Eq. (A.7)-(A.9).

$$
x^{\alpha} = \frac{N^{\alpha} \Omega}{V_0 \phi^{\alpha}} \text{ and } x^{\beta} = \frac{N^{\beta} \Omega}{V_0 \phi^{\beta}} \tag{A.7}
$$

where Ω is the volume of the crystal per Lithium site.

Partial derivative of Eq. (A.7) is

$$
\frac{\partial x^{\alpha}}{\partial N^{\alpha}} = \frac{\Omega}{V_0 \phi^{\alpha}} \text{ and } \frac{\partial x^{\beta}}{\partial N^{\alpha}} = -\frac{\Omega}{V_0 \phi^{\beta}} \tag{A.8}
$$

Also from Eq. (2.3), it is clear that

$$
\frac{\partial \varepsilon_i^{\gamma}}{\partial \varepsilon_i^{0\gamma}} = -1 \tag{A.9}
$$

where $\gamma=\alpha, \beta$ and i=2, 3.

Applying Eq. (A.7)-(A.9) to Eq. (A.6) results in

$$\begin{aligned}
&\frac{\partial g^{\alpha}}{\partial x^{\alpha}}-\frac{\partial g^{\beta}}{\partial x^{\beta}} \\
&+\frac{\Omega}{2}\left[\left(\varepsilon_2^{\alpha}\right)^2\frac{\partial \tilde{c}_{22}^{\alpha}}{\partial x^{\alpha}}+2(\varepsilon_2^{\alpha}\cdot\varepsilon_3^{\alpha})\frac{\partial \tilde{c}_{23}^{\alpha}}{\partial x^{\alpha}}+\left(\varepsilon_3^{\alpha}\right)^2\frac{\partial \tilde{c}_{33}^{\alpha}}{\partial x^{\alpha}}\right] \\
&-\frac{\Omega}{2}\left[\left(\varepsilon_2^{\beta}\right)^2\frac{\partial \tilde{c}_{22}^{\beta}}{\partial x^{\beta}}+2(\varepsilon_2^{\beta}\cdot\varepsilon_3^{\beta})\frac{\partial \tilde{c}_{23}^{\beta}}{\partial x^{\beta}}+\left(\varepsilon_3^{\alpha}\right)^2\frac{\partial \tilde{c}_{33}^{\beta}}{\partial x^{\beta}}\right] \\
&-\Omega\left[\left(\frac{\partial e^{\alpha}}{\partial \varepsilon_2^{\alpha}}\frac{\partial \varepsilon_2^{0\alpha}}{\partial x^{\alpha}}\right)+\left(\frac{\partial e^{\alpha}}{\partial \varepsilon_3^{\alpha}}\frac{\partial \varepsilon_3^{0\alpha}}{\partial x^{\alpha}}\right)\right] \\
&+\Omega\left[\left(\frac{\partial e^{\beta}}{\partial \varepsilon_2^{\beta}}\frac{\partial \varepsilon_2^{0\beta}}{\partial x^{\beta}}\right)+\left(\frac{\partial e^{\beta}}{\partial \varepsilon_3^{\beta}}\frac{\partial \varepsilon_3^{0\beta}}{\partial x^{\beta}}\right)\right]=0
\end{aligned} \tag{A.10}$$

By arranging terms in Eq. (A.10), we get

$$\begin{aligned}
&\frac{\partial g^{\alpha}}{\partial x^{\alpha}}+\frac{\Omega}{2}\left[\left(\varepsilon_2^{\alpha}\right)^2\frac{\partial \tilde{c}_{22}^{\alpha}}{\partial x^{\alpha}}+2(\varepsilon_2^{\alpha}\cdot\varepsilon_3^{\alpha})\frac{\partial \tilde{c}_{23}^{\alpha}}{\partial x^{\alpha}}+\left(\varepsilon_3^{\alpha}\right)^2\frac{\partial \tilde{c}_{33}^{\alpha}}{\partial x^{\alpha}}\right]-\Omega\left[\left(\frac{\partial e^{\alpha}}{\partial \varepsilon_2^{\alpha}}\frac{\partial \varepsilon_2^{0\alpha}}{\partial x^{\alpha}}\right)+\left(\frac{\partial e^{\alpha}}{\partial \varepsilon_3^{\alpha}}\frac{\partial \varepsilon_3^{0\alpha}}{\partial x^{\alpha}}\right)\right] \\
&=\frac{\partial g^{\beta}}{\partial x^{\beta}}+\frac{\Omega}{2}\left[\left(\varepsilon_2^{\beta}\right)^2\frac{\partial \tilde{c}_{22}^{\beta}}{\partial x^{\beta}}+2(\varepsilon_2^{\beta}\cdot\varepsilon_3^{\beta})\frac{\partial \tilde{c}_{23}^{\beta}}{\partial x^{\beta}}+\left(\varepsilon_3^{\alpha}\right)^2\frac{\partial \tilde{c}_{33}^{\beta}}{\partial x^{\beta}}\right]-\Omega\left[\left(\frac{\partial e^{\beta}}{\partial \varepsilon_2^{\beta}}\frac{\partial \varepsilon_2^{0\beta}}{\partial x^{\beta}}\right)+\left(\frac{\partial e^{\beta}}{\partial \varepsilon_3^{\beta}}\frac{\partial \varepsilon_3^{0\beta}}{\partial x^{\beta}}\right)\right]
\end{aligned} \tag{A.11}$$

So the first equilibrium condition is derived as Eq. (2.16).

$$\tilde{\mu}^{\alpha}=\tilde{\mu}^{\beta} \tag{2.16}$$

where

$$\tilde{\mu}^{\xi} = \frac{\partial g^{\xi}}{\partial x^{\xi}} + \frac{\Omega}{2}\left[\left(\varepsilon_2^{\xi}\right)^2 \frac{\partial \tilde{c}_{22}^{\xi}}{\partial x^{\xi}} + 2\left(\varepsilon_2^{\xi} \cdot \varepsilon_3^{\xi}\right)\frac{\partial \tilde{c}_{23}^{\xi}}{\partial x^{\xi}} + \left(\varepsilon_3^{\xi}\right)^2 \frac{\partial \tilde{c}_{33}^{\xi}}{\partial x^{\xi}}\right] - \Omega \sum_{i=2}^{3} \frac{\partial e^{\xi}}{\partial \varepsilon_i^{\xi}} \frac{\partial \varepsilon_i^{0\xi}}{\partial x^{\xi}} \tag{2.21}$$

where $\xi=\alpha, \beta$.

2nd equilibrium condition is

$$\left(\frac{\partial G}{\partial \phi^{\alpha}}\right)_{N^{\alpha}, \tilde{\varepsilon}_2, \tilde{\varepsilon}_3} = 0 \tag{2.13}$$

Having $x^{\beta} = x^{\beta}(x^{\alpha}, \phi^{\alpha})$ in mind, we expand Eq. (2.13).

$$Mg^{\alpha} + V_0 e^{\alpha} - Mg^{\beta} - V_0 e^{\beta} + M\phi^{\beta} \frac{\partial g^{\beta}}{\partial x^{\beta}} \frac{\partial x^{\beta}}{\partial \phi^{\alpha}} + V_0 \phi^{\beta} \frac{\partial e^{\beta}}{\partial x^{\beta}} \frac{\partial x^{\beta}}{\partial \phi^{\alpha}} = 0 \tag{A.12}$$

By dividing Eq. (A.12) by M and expanding further, we get

$$\begin{aligned} &\tilde{g}^{\alpha} - \tilde{g}^{\beta} + \phi^{\beta} \frac{\partial g^{\beta}}{\partial x^{\beta}} \frac{\partial x^{\beta}}{\partial \phi^{\alpha}} \\ &+\Omega\phi^{\beta} \frac{\partial x^{\beta}}{\partial \phi^{\alpha}}\left[\frac{1}{2}\left(\left(\varepsilon_2^{\beta}\right)^2 \frac{\partial \tilde{c}_{22}^{\beta}}{\partial x^{\beta}} + 2(\varepsilon_2^{\beta} \cdot \varepsilon_3^{\beta})\frac{\partial \tilde{c}_{23}^{\beta}}{\partial x^{\beta}} + \left(\varepsilon_3^{\alpha}\right)^2 \frac{\partial \tilde{c}_{33}^{\beta}}{\partial x^{\beta}}\right) - \left(\frac{\partial e^{\beta}}{\partial \varepsilon_2^{\beta}} \frac{\partial \varepsilon_2^{0\beta}}{\partial x^{\beta}}\right) - \left(\frac{\partial e^{\beta}}{\partial \varepsilon_3^{\beta}} \frac{\partial \varepsilon_3^{0\beta}}{\partial x^{\beta}}\right)\right] = 0 \end{aligned} \tag{A.13}$$

From the definition of Lithium chemical potential in Eq. (2.21), Eq. (A.13) is simplified to

$$\tilde{g}^{\alpha} - \tilde{g}^{\beta} + \phi^{\beta} \frac{\partial x^{\beta}}{\partial \phi^{\alpha}} \tilde{\mu}^{\beta} = 0 \tag{A.14}$$

By substituting the partial differential in Eq. (A.14), we get

$$\tilde{g}^{\alpha} - \tilde{g}^{\beta} + \phi^{\beta} \tilde{\mu}^{\beta} \frac{x - x^{\alpha}}{\left(\phi^{\beta}\right)^{2}} = 0 \tag{A.15}$$

Further manipulation is shown in Eq. (A.16) - (A.18).

$$\tilde{g}^{\alpha} - \tilde{g}^{\beta} + \tilde{\mu}^{\beta} \frac{x^{\beta}\phi^{\beta} + (\phi^{\alpha} - 1)x^{\alpha}}{\phi^{\beta}} = 0 \tag{A.16}$$

$$\tilde{g}^{\alpha} + \frac{(\phi^{\alpha} - 1)x^{\alpha}}{\phi^{\beta}} = \tilde{g}^{\beta} - x^{\beta}\tilde{\mu}^{\beta} \tag{A.17}$$

$$\tilde{g}^{\alpha} - x^{\alpha}\tilde{\mu}^{\beta} = \tilde{g}^{\beta} - x^{\beta}\tilde{\mu}^{\beta} \tag{A.18}$$

By applying first equilibrium criteria in Eq. (2.16) to Eq. (A.18), we get

$$\tilde{g}^{\alpha} - x^{\alpha}\tilde{\mu}^{\alpha} = \tilde{g}^{\beta} - x^{\beta}\tilde{\mu}^{\beta} \tag{A.19}$$

third and fourth minimum conditions lead to mechanical equilibrium criteria. They will be dealt together below.

$$\left(\frac{\partial G}{\partial \tilde{\varepsilon}_2^{\alpha}}\right)_{N^{\alpha},\phi^{\alpha},\tilde{\varepsilon}_3} = 0 \tag{2.14}$$

$$\left(\frac{\partial G}{\partial \tilde{\varepsilon}_3^{\alpha}}\right)_{N^{\alpha},\phi^{\alpha},\tilde{\varepsilon}_2} = 0 \tag{2.15}$$

Since the elastic energy is dependent only on strains, Eq. (2.14) and Eq. (2.15) become

$$V_0\left(\phi^{\alpha}\frac{\partial e^{\alpha}}{\partial \tilde{\varepsilon}_i} + \phi^{\beta}\frac{\partial e^{\beta}}{\partial \tilde{\varepsilon}_i}\right) = 0 \tag{A.20}$$

where *i*=2, 3.

Since the elastic strains are function of pure mechanical strains, we apply the chain rule.

$$V_0\left(\phi^{\alpha}\frac{\partial e^{\alpha}}{\partial \varepsilon_i}\frac{\partial \varepsilon_i}{\partial \tilde{\varepsilon}_i} + \phi^{\beta}\frac{\partial e^{\beta}}{\partial \varepsilon_i}\frac{\partial \varepsilon_i}{\partial \tilde{\varepsilon}_i}\right) = 0 \tag{A.21}$$

Because the total strain is

$$\tilde{\varepsilon}_i = \varepsilon_i^{o\gamma}(N^{\alpha}) + \varepsilon_i \tag{A.22}$$

, partial differentiation of Eq. (A.22) is obvious:

$$\left(\frac{\partial \varepsilon_i}{\partial \tilde{\varepsilon}_i}\right)_{N^\alpha} = 1 \tag{A.23}$$

Applying Eq. (A.23) and partial differentiation of Eq. (2.6) to Eq. (A.21), we get

$$V_0\left(\phi^\alpha \frac{\partial e^\alpha}{\partial \varepsilon_i} + \phi^\beta \frac{\partial e^\beta}{\partial \varepsilon_i}\right) = V_0\left(\phi^\alpha \sigma_i^\alpha + \phi^\beta \sigma_i^\beta\right) = 0 \tag{A.24}$$

As a result, the mechanical equilibrium criteria are derived.

$$\phi^\alpha \sigma_2^\alpha + \phi^\beta \sigma_2^\beta = 0 \tag{2.18}$$

$$\phi^\alpha \sigma_3^\alpha + \phi^\beta \sigma_3^\beta = 0 \tag{2.19}$$

A. 3. Total Strain Derivation

I will show detailed calculation for the total strain in Chapter II, which is

$$\tilde{\varepsilon}_i = \tau_i x \tag{2.26}$$

From the assumption that elastic moduli are independent of Lithium concentration and the lattice parameters obey Vegrard's law, a solution to the mechanical equilibrium criteria is possible without considering the chemical equilibrium criteria. The mechanical equilibrium criteria is

$$\phi^{\alpha}\sigma_2^{\alpha} + \phi^{\beta}\sigma_2^{\beta} = 0 \tag{2.18}$$

$$\phi^{\alpha}\sigma_3^{\alpha} + \phi^{\beta}\sigma_3^{\beta} = 0 \tag{2.19}$$

Since $\sigma_2^{\gamma} = \tilde{c}_{22}\varepsilon_2^{\gamma} + \tilde{c}_{23}\varepsilon_3^{\gamma}$ and $\sigma_3^{\gamma} = \tilde{c}_{32}\varepsilon_2^{\beta} + \tilde{c}_{33}\varepsilon_3^{\beta}$, Eq. (2.18) and (2.19) can be written as

$$\begin{aligned}\phi^{\alpha}(\tilde{c}_{32}\varepsilon_2^{\alpha} + \tilde{c}_{33}\varepsilon_3^{\alpha}) + \phi^{\beta}(\tilde{c}_{32}\varepsilon_2^{\beta} + \tilde{c}_{33}\varepsilon_3^{\beta}) = 0\\ \phi^{\alpha}(\tilde{c}_{22}\varepsilon_2^{\alpha} + \tilde{c}_{23}\varepsilon_3^{\alpha}) + \phi^{\beta}(\tilde{c}_{22}\varepsilon_2^{\beta} + \tilde{c}_{23}\varepsilon_3^{\beta}) = 0\end{aligned} \tag{A.25}$$

which can be rewritten as

$$\begin{aligned}\tilde{c}_{22}(\phi^{\alpha}\varepsilon_2^{\alpha} + \phi^{\beta}\varepsilon_2^{\beta}) + \tilde{c}_{23}(\phi^{\alpha}\varepsilon_3^{\alpha} + \phi^{\beta}\varepsilon_3^{\beta}) = 0\\ \tilde{c}_{32}(\phi^{\alpha}\varepsilon_2^{\alpha} + \phi^{\beta}\varepsilon_2^{\beta}) + \tilde{c}_{33}(\phi^{\alpha}\varepsilon_3^{\alpha} + \phi^{\beta}\varepsilon_3^{\beta}) = 0\end{aligned} \tag{A.26}$$

Since Eq. (A.26) should be satisfied with any elastic moduli, we find

$$\begin{aligned}\phi^{\alpha}\varepsilon_2^{\alpha} + \phi^{\beta}\varepsilon_2^{\beta} = 0\\ \phi^{\alpha}\varepsilon_3^{\alpha} + \phi^{\beta}\varepsilon_3^{\beta} = 0\end{aligned} \tag{A.27}$$

Applying the relation of total strain Eq. (2.3) to Eq. (A.27), we get

$$\begin{aligned}\phi^{\alpha}(\tilde{\varepsilon}_2^{\alpha} - \varepsilon_2^{0\alpha}) + \phi^{\beta}(\tilde{\varepsilon}_2^{\beta} - \varepsilon_2^{0\beta}) = \phi^{\alpha}(\tilde{\varepsilon}_2^{\alpha} - \tau_2 x^{\alpha}) + \phi^{\beta}(\tilde{\varepsilon}_2^{\beta} - \tau_2 x^{\beta}) = 0\\ \phi^{\alpha}(\tilde{\varepsilon}_3^{\alpha} - \varepsilon_3^{0\alpha}) + \phi^{\beta}(\tilde{\varepsilon}_3^{\beta} - \varepsilon_3^{0\beta}) = \phi^{\alpha}(\tilde{\varepsilon}_3^{\alpha} - \tau_3 x^{\alpha}) + \phi^{\beta}(\tilde{\varepsilon}_3^{\beta} - \tau_3 x^{\beta}) = 0\end{aligned} \tag{A.28}$$

Since $\tilde{\varepsilon}_i^{\alpha} = \tilde{\varepsilon}_i^{\beta} (= \tilde{\varepsilon}_i)$ from coherency constraint, Eq. (A.28) can be written as

$$\begin{aligned} (\phi^{\alpha} + \phi^{\beta})\tilde{\varepsilon}_2 &= -\tau_2(\phi^{\beta} x^{\alpha} + \phi^{\beta} x^{\beta}) \\ (\phi^{\alpha} + \phi^{\beta})\tilde{\varepsilon}_3 &= -\tau_3(\phi^{\beta} x^{\alpha} + \phi^{\beta} x^{\beta}) \end{aligned} \tag{A.29}$$

To simplify Eq. (A.29), we use the properties of total concentration and sum of phase fractions below in Eq (A.30) and Eq. (A.31).

$$x^{\alpha}\phi^{\alpha} + x^{\beta}\phi^{\beta} = x \tag{A.30}$$

$$\phi^{\alpha} + \phi^{\beta} = 1 \tag{A.31}$$

As a result, the total strains in second and third direction can be written as Eq. (2.26).

$$\tilde{\varepsilon}_i = \tau_i x \tag{2.26}$$

BIBLIOGRAPHY

Bibliography

[1] A. Pantano and R. C. Averill, "A penalty-based finite element interface technology," *Computers and Structures,* 2002.

[2] M. M. Thackeray, "Manganese oxides for lithium batteries," *Progress in Solid State Chemistry,* vol. 25, pp. 1-71, 1997.

[3] M. S. Whittingham*, et al.*, "Introduction: Batteries and fuel cells," *Chemical Reviews,* vol. 104, pp. 4243-4244, Oct 2004.

[4] J. M. Tarascon and M. Armand, "Issues and challenges facing rechargeable lithium batteries," *Nature,* vol. 414, pp. 359-367, Nov 15 2001.

[5] A. Van der Ven and G. Ceder, "Lithium diffusion mechanisms in layered intercalation compounds," *Journal of Power Sources,* vol. 97, pp. 529-531, 2001.

[6] A. Van der Ven*, et al.*, "Nondilute diffusion from first principles: Li diffusion in Li_xTiS_2," *Physical Review B,* vol. 78, p. 104306, 2008.

[7] G. Chen*, et al.*, "Electron Microscopy Study of the $LiFePO_4$ to $FePO_4$ Phase Transition," *Electrochemical and solid-state letters,* vol. 9, p. A295, 2006.

[8] J. A. Sethian, *Level set methods: evolving interfaces in geometry, fluid mechanics, computer vision, and materials science*, 1996.

[9] D. Morgan*, et al.*, "Li Conductivity in LiMPO (M= Mn, Fe, Co, Ni) Olivine Materials," *Electrochemical and solid-state letters,* vol. 7, p. A30, 2004.

[10] R. B. Schwarz and A. G. Khachaturyan, "Thermodynamics of Open 2-Phase Systems with Coherent Interfaces," *Physical Review Letters,* vol. 74, pp. 2523-2526, Mar 27 1995.

[11] R. B. Schwarz and A. G. Khachaturyan, "Thermodynamics of open two-phase systems with coherent interfaces: Application to metal-hydrogen systems," *Acta Materialia,* vol. 54, pp. 313-323, Jan 2006.

[12] A. Van der Ven, "The role of coherency strains on phase stability in Li_xFePO_4: needle crystallites minimize coherency strain and overpotential," *Journal of the Electrochemical Society,* vol. 156, 2009.

[13] T. Maxisch and G. Ceder, "Elastic properties of olivine Li_xFePO_4 from first principles," *Physical Review B,* vol. 73, p. 174112, 2006.

[14] M. Hillert, *Phase equilibria, phase diagrams, and phase transformations : their thermodynamic basis*. Cambridge, U.K. ; New York: Cambridge University Press, 1998.

[15] F. Zhou*, et al.*, "Configurational electronic entropy and the phase diagram of mixed-valence oxides: The case of LixFePO4," *Physical Review Letters,* vol. 97, pp. -, Oct 13 2006.

[16] N. Meethong*, et al.*, "Electrochemically Induced Phase Transformation in Nanoscale Olivines $Li_{1-x}MPO_4$ (M = Fe, Mn)," *Chemistry of Materials,* vol. 20, pp. 6189-6198, Oct 14 2008.

[17] A. R. Denton and N. W. Ashcroft, "Vegard Law," *Physical Review A,* vol. 43, pp. 3161-3164, Mar 15 1991.

[18] M. S. Whittingham*, et al.*, "Some transition metal (oxy)phosphates and vanadium oxides for lithium batteries," *Journal of Materials Chemistry,* vol. 15, pp. 3362-3379, 2005.

[19] E. Olsson*, et al.*, "A conservative level set method for two phase flow II," *Journal of Computational Physics,* vol. 225, pp. 785-807, 2007.

[20] V. Rao*, et al.*, "On modelling thermal oxidation of Silicon II: numerical aspects," *International Journal for Numerical Methods in Engineering,* vol. 47, pp. 359-377, 2000.

[21] J. Donéa and A. Huerta, *Finite element methods for flow problems*. Chichester ; Hoboken, NJ: Wiley, 2003.

[22] B. Cockburn*, et al.*, *Discontinuous Galerkin methods : theory, computation, and applications*. Berlin ; New York: Springer, 2000.

[23] J. C. Simo and F. Armero, "Geometrically Nonlinear Enhanced Strain Mixed Methods and the Method of Incompatible Modes," *International Journal for Numerical Methods in Engineering,* vol. 33, pp. 1413-1449, May 30 1992.